

NEW HIGH PROPER MOTION STARS FROM THE DIGITIZED SKY SURVEY. IV. COMPLETION OF THE SOUTHERN SURVEY AND 170 ADDITIONAL STARS WITH $\mu > 0.45''\text{YR}^{-1}$.¹

SÉBASTIEN LÉPINE

Department of Astrophysics, Division of Physical Sciences, American Museum of Natural History, Central Park West at 79th Street, New York, NY 10024, USA

To appear in the Astronomical Journal

ABSTRACT

Completion of the SUPERBLINK proper motion survey in the southern celestial hemisphere has turned up 170 new stars with proper motion $0.45''\text{yr}^{-1} < \mu < 2.0''\text{yr}^{-1}$. This fourth and final installment completes the all-sky, data-mining of the Digitized Sky Surveys for stars with large proper motions. The areas investigated in this final installment comprise 11,600 square degrees in the declination range $-30^\circ < \text{Decl.} < 0^\circ$ and in low galactic latitude areas south of $\text{Decl.} = -30^\circ$ which had not been covered in earlier data releases. Astrometric and photometric data are provided for the 170 new stars, along with finder charts. Most of the new discoveries are found in densely populated fields along the Milky Way, towards the Galactic bulge/center. The list of new discoveries includes 4 stars with proper motion $\mu > 1.0''\text{yr}^{-1}$. The total list of high proper motion stars recovered by SUPERBLINK in the southern sky now includes 2,228 stars with proper motions $0.45''\text{yr}^{-1} < \mu < 2.0''\text{yr}^{-1}$.

Subject headings: astrometry — surveys — stars: kinematics — solar neighborhood — binaries: visual — stars: white dwarfs

1. INTRODUCTION

The search for stars with large proper motions has been a key research area for stellar astrophysics in the past century. Large-scale surveys of high proper motion (HPM) stars have been instrumental in mapping out the Solar Neighborhood, determining the kinematics of local stellar populations, and evaluating the stellar contents of the Galaxy. Classes of low-luminosity field stars, such as red dwarfs, white dwarfs, and cool subdwarfs, have been first identified from catalogs of high proper motion objects.

The bulk of all known stars with large proper motions was discovered and cataloged in the course of two massive, dedicated proper motion surveys carried out in the 1960s and 1970s. The first one is the Lowell Proper Motion Survey, performed using the 13-inch photographic telescope of the Lowell Observatory, using 1930s plates as a first epoch. Stars with proper motions $> 0.25''\text{yr}^{-1}$ identified in the survey are listed in a catalog of 8,991 objects in the northern sky (Giclas, Burnham, & Thomas 1971), and a catalog of 2,758 objects in the southern sky (Giclas, Burnham, & Thomas 1978). The second large proper motion survey is the one carried out by W. J. Luyten, which used the 1950s National Geographic Palomar Sky Survey as a first epoch, and a set of duplicate plates which Luyten obtained at Palomar in the 1960s. Stars with proper motions larger than $0.18''\text{yr}^{-1}$ were published in the “NLTT catalog” (Luyten 1979a), with compiles 58,845 individual objects. The “LHS catalog”, essentially a subset of the NLTT, listed stars with proper motions $\mu > 0.50''\text{yr}^{-1}$, with 4,470 entries. But for a few exceptions, all the stars from the Lowell Proper Motion Survey were also listed in the Luyten catalogs. Assembled before the generalized use of computers, with records written by hand and typewritten, the NLTT and LHS cata-

logs had recorded positional accuracies of several arcseconds (Gould & Salim 2003) and also contained a small but significant number of typos (Lépine, Shara, & Rich 2002). Several efforts have been made to revise the positions of the NLTT and LHS stars, and refine the accuracy of their astrometric and photometric measurements (Bakos, Sahu, & Nemeth 2002; Salim & Gould 2003) often to find some stars off their recorded position by one arcminute or more.

The main limitation of the Luyten catalogs, however, was its obvious incompleteness in specific areas of the sky (Dawson 1986). The NLTT/LHS catalogs were notably incomplete in low galactic latitude areas, where the high stellar density the identification of HPM stars very challenging using the traditional blink-comparator method. The Luyten survey was also notably incomplete in areas south of $\text{Decl.} = -30^\circ$, which could not be imaged from Palomar Observatory, from where Luyten obtained his second epoch plates. The known incompleteness of the Luyten catalogs at southern declinations has motivated most subsequent investigators to concentrate on the southern sky. While the LHS/NLTT catalogs were largely complete on the bright end ($V < 15$) the potential for spectacular discoveries at the faint end, such as very low-mass stars and brown dwarfs in the immediate proximity of the Sun, or high-velocity halo white dwarfs, was also a strong motivation for performing more systematic and sensitive surveys of high proper motion stars over the entire sky.

In the past 10 years, a succession of proper motion surveys, covering a patchwork of southern sky areas, have been regularly supplying lists of new HPM stars, slowly increasing the completeness of the all-sky census. First, a survey of 131 scattered areas covering about 3,200 square degrees of the southern sky, was conducted by Wroblewski & Torres (1997) and Wroblewski & Costa (2001). The new survey identified 1,642 new proper motion stars, including 50 with $\mu > 0.5''\text{yr}^{-1}$. The survey was based on a visual comparison of pairs of photographic plates on a Zeiss-Jena blink comparator.

A smaller survey, known as the Calán-ESO (CE) Proper

¹ Based on data mining of the Digitized Sky Survey, developed and operated by the Catalogs and Surveys Branch of the Space Telescope Science Institute, Baltimore, USA.

Motion Survey (Ruiz *et al.* 2001), examined 325 square degrees of the southern sky in much detail. The survey recovered 542 objects, including 385 new high proper motion stars², of which 14 have $\mu > 0.5'' \text{ yr}^{-1}$. The survey was also based on direct visual comparison of plate pairs using a blink machine. The survey is famous for its discovery of Kelu-1, the first L dwarf found in isolation (Ruiz, Leggett, & Allard 1997).

The APM proper motion survey of the southern sky was initiated by (Scholz *et al.* 2000), focusing on the identification of stars with $0.3'' \text{ yr}^{-1} < \mu < 1.0'' \text{ yr}^{-1}$. This survey was based on a re-analysis of scans of UK Schmidt plates with the Cambridge APM machine. Results have however not been published consistently, and some stars from the survey (APMPM stars) have appeared in the literature only after follow-up spectroscopic observations (Reylé *et al.* 2002).

The Liverpool-Edinburgh high proper motion survey (LEHPM) covered over 3,000 square degrees of sky near the south Galactic cap. The survey was based on an analysis of star positions, measured with SuperCOSMOS, in 31 fields from the R-band (IIIaF) ESO and UK Schmidt Plates. The survey yielded 6,206 detections of stars with proper motion $\mu > 0.2'' \text{ yr}^{-1}$ (Pokorny, Jones, & Hambly 2003). About half of the detections did not correspond to stars previously reported in the literature, including a possible 92 new stars with proper motions $\mu > 0.5'' \text{ yr}^{-1}$. Some of the new objects reported in the LEHPM are however suspected to be spurious (Subasavage, *et al.* 2005a).

The SuperCOSMOS-RECONS proper motion survey was also based on data-mining of the SuperCOSMOS Sky Survey, and extended over most of the southern sky, only excluding some areas at low Galactic latitudes. The survey was especially productive, leading to the discovery of 307 new stars with proper motion $\mu > 0.4'' \text{ yr}^{-1}$, including 150 with $\mu > 0.5'' \text{ yr}^{-1}$ (Subasavage, *et al.* 2005a,b).

Finally, the Southern Infrared Proper Motion Survey (SIPS) has been probing the entire southern sky based on a comparison of SuperCOSMOS Sky Survey against the 2MASS All-Sky Catalog, used as a second epoch (Deacon, Hambly, & Cooke 2005). Thus far, 144 high proper motion stars have been reported, all with $\mu > 0.5'' \text{ yr}^{-1}$, including 70 new discoveries. Because it uses infrared data, the survey is most sensitive to cool, very low mass stars and brown dwarfs.

In the past 7 years, we have been conducting our own survey for stars with high proper motions, with the aim of covering the entire sky, and at the highest possible completeness rate. The SUPERBLINK proper motion survey is based on a re-analysis of the Digitized Sky Surveys using an image-differencing technique. The survey was first conducted over the entire northern sky, before being extended to the southern hemisphere. At northern declinations, we discovered 198 new stars with proper motions $\mu > 0.5'' \text{ yr}^{-1}$ (Lépine, Shara, & Rich 2002, 2003), the largest such finding since the catalogs of Luyten. With the publication of the LSPM-north catalog of stars with proper motions $\mu > 0.15'' \text{ yr}^{-1}$ (Lépine, & Shara 2005), the census of the northern sky is now considered to be 99% complete at high galactic lati-

tude ($\|b\| > 15^\circ$) and 90% complete at low galactic latitude ($\|b\| < 15^\circ$), for HPM stars down to a visual magnitude of 19. In the northern sky, the LSPM-north catalog now effectively supersedes the Luyten catalogs, and should now serve as the primary database for stars with large proper motions.

The SUPERBLINK survey now extends over most of the southern sky as well. In the third paper of this series, we reported the discovery of 182 new stars with proper motions $\mu > 0.45'' \text{ yr}^{-1}$, all discovered south of Decl. $=-30^\circ$. In this fourth and final paper of the series, we report the discovery of an additional 170 new stars with proper motions in the range $0.45'' \text{ yr}^{-1} < \mu < 2.00'' \text{ yr}^{-1}$, identified in the final survey area covering the remaining $\approx 12,000$ square degrees of southern sky. This fourth list of objects completes our all-sky search for stars with very large proper motions in the Digitized Sky Surveys.

2. SEARCH AND IDENTIFICATION

High proper motion stars were identified from data-mining of the Digitized Sky Surveys using the SUPERBLINK software. The method has been described in much detail in Papers I-III of this series (Lépine, Shara, & Rich 2002, 2003; Lépine 2005) and the accuracy and completeness of the technique, for the northern sky survey, has been documented in Lépine, & Shara (2005). The method is based on an image subtraction algorithm, which emphasizes objects that have moved significantly between any two epochs of photographic images. The software generates lists of possible moving objects along with two-epoch finder charts. These charts are blinked on the computer screen for quality control. All objects with very large proper motions detected by SUPERBLINK are thus verified by a human eye, which minimizes contamination by any of several kinds of spurious objects due to plate defects and other artifacts.

The SUPERBLINK software works by comparing pairs of images obtained at different epochs. The efficiency in detecting high proper motion stars depends on the time difference between the two images; a longer temporal baseline will yield a higher accuracy on proper motion measurements, and an increased sensitivity to stars with smaller proper motions. The method also works best for fields of similar appearance and quality (dynamical range, magnitude limit, seeing). Ideally, the fields should have been imaged in similar passbands and with comparable exposure times. This needs not strictly be the case, however, since SUPERBLINK includes algorithms which adjust intensity levels and use convolutions to match the quality of the two images as best as possible.

The Digitized Sky Surveys (DSS) covers every part of the sky in at least 2 different epochs and in various passbands (blue, red, infrared). In the northern sky, the DSS has full coverage at two different epochs with sets of red plates, and with a temporal baseline ~ 40 years. These are the data we have used in the north. In the southern sky, however, the DSS does not provide full coverage at two epoch *and* in the same passband. To get full coverage at two epochs, one has to use pairs of plates imaged in different passbands.

For about half of the southern sky, in the declination range $-30^\circ < \text{Decl.} < 0^\circ$, scans from the first Palomar Sky Survey (POSS-I) are available in both blue (103aO) and red (103aE) passbands, all imaged between 1950 to 1958. The red POSS-I scans have been used as a first epoch against scans from the red (IIIaF) Second Epoch Southern and Equatorial Red surveys, which cover the same area and were imaged between 1984 and 1998. The temporal baseline between the first and

² The text of the (Ruiz *et al.* 2001) paper mentions 154 stars previously listed in the Luyten catalogs, however their table 2 clearly lists 157 stars with NLTT/LHS identifiers, from which we obtain the number of 385 new high proper motion stars.

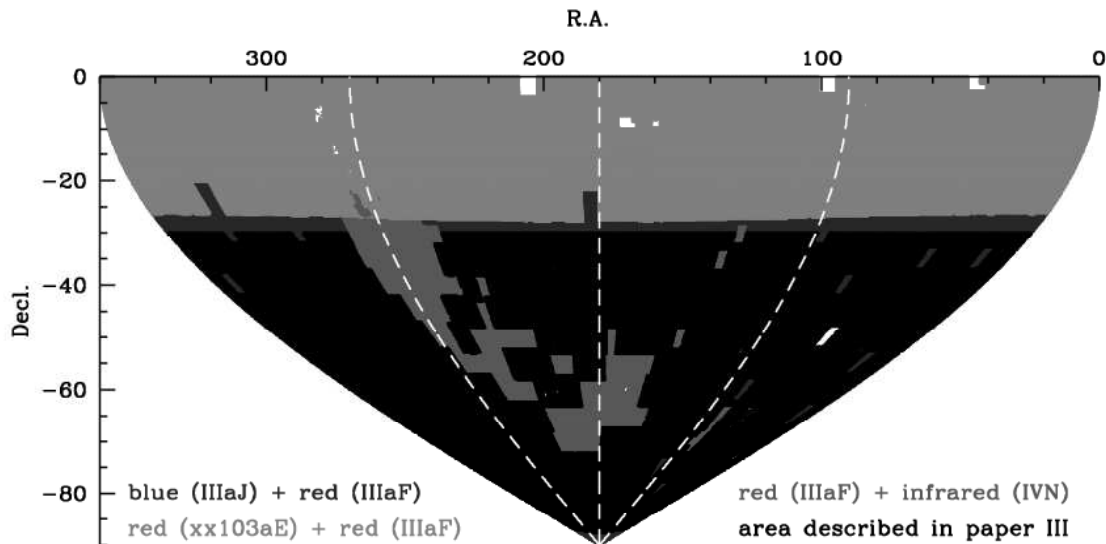


FIG. 1.— Areas of the southern sky searched by the SUPERBLINK software for stars with large proper motions. Regions shaded in black indicate areas that were analyzed for Paper III; areas analyzed for this paper are shaded in color. In green are regions for which we used Digitized Sky Surveys scans of red plates (103aE, IIIaF) for both the first and second epochs. Areas in blue denote regions where scans from blue plates (IIIaJ) were used for the first epochs, and scans from red plates (IIIaF) for the second epochs. Areas in red are those for which scans of infrared plates (IVn) were used as first epoch against red plates (IIIaF) for the second epoch. The survey overall covers 97.2% of the southern sky.

second epoch varied between 27 and 47 years. The area covered by those plate pairs is shown in Figure 1, shaded in green.

To complete the survey down to $\text{Decl.} = -30^\circ$, we used the same strategy as described in Paper III (for the sky south of -30°): we used scans from the SERC-J survey as the first epoch. These scans consist in blue (IIIaJ) plates obtained between 1974 and 1986. The SERC-J scans were matched against red (IIIaF) Second Epoch Southern survey (SES) scans, which consist in plates imaged between 1987 and 1998. The SES plates yields temporal baselines between 3 and 21 years, with a median of 15 years. As explained in Paper III, the software has the capability of matching the counterparts of moving stars from first and second epoch images of different colors. The counterparts need not have exactly the same plate magnitude in both images, though a large difference due to e.g. an extreme color, will make the detection more difficult. Figure 1 displays (shaded in blue) the area of the sky where such blue/red plate pairs had to be used. Areas analyzed in Paper III, using the same strategy, are shaded in black. Thirteen additional areas south of $\text{Decl.} = -30^\circ$ which had not been analyzed in Paper III have been added here (also shaded in blue).

Finally, there remained areas for which no suitable first epoch images could be found from either red or blue photographic plates. These included a large swath of the sky at low galactic latitude, especially pointings towards the Galactic bulge, and also plates covering the Large Magellanic cloud. For those areas, we had to use as first epoch scans from the SERC-I survey, which are photographic infrared plates obtained with the IVN emulsion, and imaged between 1978 and 1988. These were matched against scans from the red (IIIaF) Second Epoch Southern survey, from plates shot between 1989 and 1996. The temporal baseline in these red/infrared plate pairs was between 3 and 17 years, with a 12 years median.

The southern sky was divided in 615,900 areas, each one

a square subfield $17' \times 17'$ in extent. The subfields were spaced out on a $15' \times 15'$ grid, allowing for significant overlap between neighboring subfields. SUPERBLINK successfully processed 598,712 subfields, or 97.2% of the total survey area. Some 17,188 subfields were left unprocessed by SUPERBLINK, after the software failed to properly align the corresponding first and second epoch images. This typically occurs in subfields containing very bright ($V < 5$) stars, which saturate the plate over an extended patch of sky, over which no reference sources can be used for aligning the first and second epoch images. Some extremely dense fields near the Galactic center and in the Magellanic clouds likewise could not be processed because of extensive plate saturation. Additional pairs of first and second epoch images could also not be properly superposed by the software because the software could not match the first and second epoch subfields because of significant differences between them, either because of large differences in the seeing, or significant differences in plate depth.

High proper motion stars were identified in all three sets of plates pairs (red/red, blue/red, red/infrared) in roughly equivalent numbers of detection per unit area. We did, however, observe differences in the magnitude and color distribution of the HPM stars found in the three survey areas. Figure 2 plots the distribution in V magnitude (left panels) and $V-J$ color (right panels) for subsamples of 2,500 stars identified by SUPERBLINK in red/red, blue/red, and red/infrared plate pairs. Our general method for estimating V and $V-J$ is detailed in Lépine, & Shara (2005). Stars detected in the red/red pairs show a sharp drop in magnitude around $V=20$, which is consistent with the limiting magnitude from the northern sky survey, which was also done using red/red pairs (Lépine, & Shara 2005). The V magnitude distribution of stars from the red/infrared pairs, on the other hand, shows a sharp drop at $V=18$, suggesting that our proper motion survey is about 2 magnitudes shallower in the red/infrared areas. It is unclear how much of this is due to actual limitations from the

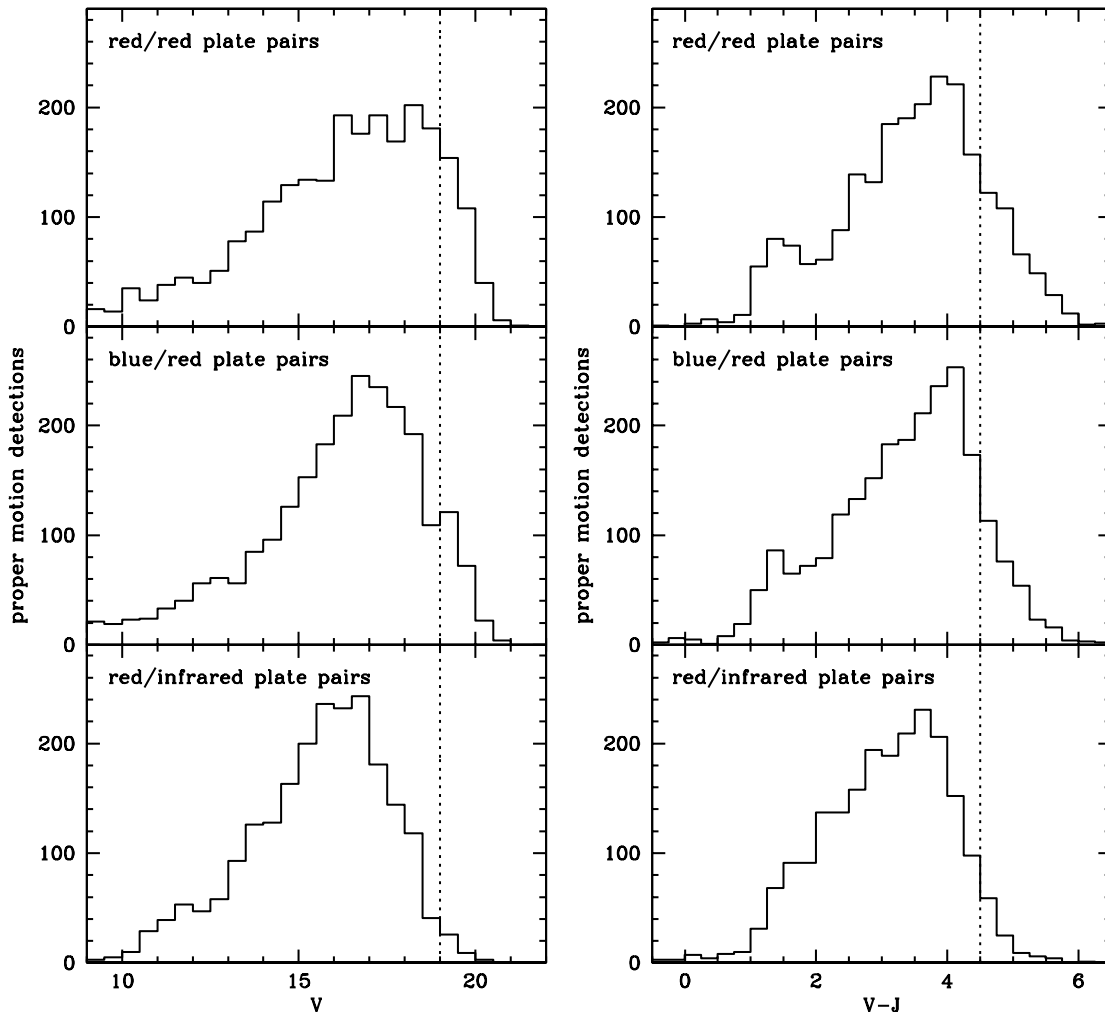


FIG. 2.— Distribution of V magnitudes and $V-J$ colors for three subsamples of 2,500 stars identified by SUPERBLINK in each of the three main survey areas: regions where scans of red (IIIaF) plates were used for both the first and second epoch images (red/red), regions where scans of blue (IIIaJ) plates were used as first epoch and scans of red plates as second epoch (blue/red), and regions where scans of red plates were used as first epoch and scans of infrared plates (IVn) were used as second epoch (red/infrared). The survey is shown to be shallower in the red/infrared areas, reaching only to $V=18$, while it is 2 magnitudes deeper in the red/red pairs. The survey also appears to be less efficient in detecting very red objects ($V-J > 4.5$) when using the blue/red and red/infrared plates.

use of the different passband red/infrared pairs, or how much could be due to the fact that most of the red/infrared pairs covered fields at low Galactic latitude, where the high density of stars makes the identification of faint moving objects more difficult. Assuming all three surveys to be effectively complete to $V = 16.0$, then the survey with the red/infrared pairs is at most 80% complete down to $V = 19.0$, lacking a significant number of the fainter ($16 < V < 19$) stars. The blue/red pairs survey is at most 95% complete down to $V = 19.0$, compared with the red/red survey.

The distributions of $V-J$ colors for stars found in the three survey areas are relatively similar over most of the $V-J$ range, which shows no major problems in selecting stars with moderate color terms in the blue/red and red/infrared plates. However, the number of HPM stars with very red colors ($V-J > 4.5$) varies significantly in the three sets. Fewer HPM stars with such red color are detected in the blue/red pairs (11%

of stars detected have $V-J > 4.5$) than in the red/red pairs (15%), and even fewer are found in the red/infrared pairs (4%). This suggests that stars with extreme colors were not consistently identified by the code in the blue/red and red/infrared pairs, most probably because of significant differences in the stars' magnitudes between the first and second epoch plates, due to the different imaging passband.

3. RECOVERY OF KNOWN HIGH PROPER MOTIONS STARS

In all areas of the southern sky analyzed with SUPERBLINK, we identified a total of 2,040 stars with proper motions $0.45'' \text{ yr}^{-1} < \mu < 2.00'' \text{ yr}^{-1}$. This number excludes all the bright stars identified by SUPERBLINK which were found listed in the TYCHO-2 catalog, which we use as a fiducial for the bright magnitude limit of our survey. The number also include 138 individual stars identified as members of common proper motions pairs (69 systems).

The complete list of non-TYCHO stars was cross-

correlated against all the historical catalogs discussed in §1. A significant fraction of the stars detected by SUPERBLINK were found listed in either one of the LHS or NLTT catalogs (1,395 stars). Of these, 234 are also listed in the Lowell southern catalog (Giclas, Burnham, & Thomas 1978). Additionally, we found a match to the star G267-073, which is listed in the Giclas catalog but not in the LHS/NLTT. Among the stars that could not be matched against the older proper motion catalogs, we found 55 matches to stars discovered in the proper motion survey of Wroblewski & Torres (1997) and Wroblewski & Costa (2001). We found another 14 stars which were discovered in the Calán-ESO Proper Motion Survey (Ruiz *et al.* 2001). Some 32 stars were first identified in the APM proper motion survey of Scholz *et al.* (2000), while 57 stars were first listed in the LEHPM proper motion catalog (Pokorny, Jones, & Hambly 2003). Yet another 180 stars were discovered by our own SUPERBLINK survey but reported in earlier papers of this series (Lépine, Shara, & Rich 2003; Lépine 2005), and 117 more stars were matches to objects first reported in the SCR survey (Subasavage, *et al.* 2005a,b). Finally, 4 more objects were first reported in the SIPS catalog (Deacon, Hambly, & Cooke 2005).

Stars not found in any of the catalogs above were then searched for possible mentions in the astronomical literature using Simbad³. The search yielded 15 more matches to known nearby or high proper motion stars. Six objects were matches to spectroscopically confirmed white dwarfs. The first one is the high proper motion white dwarf WD J0100-645 discovered by Oppenheimer *et al.* (2001) in a proper motion survey of the south Galactic cap. The second one is the high proper motion star USNO-B 0867-0249298, one of two stars with proper motion $\mu > 1.0''\text{yr}^{-1}$ confirmed by Levine (2005) in a follow-up analysis of high proper motion entries in the USNO-B1.0 catalog of Monet *et al.* (2003). The other four white dwarfs are WD 0202-055, WD 2346-478, and the common proper motion white dwarf pair of WD 2226-754 and WD 2226-755, all reported in the catalog of McCook & Sion (1999).

We also found matches to 9 objects reported in the literature as very cool, nearby stars. One was a match to APMPM J0413-3729, identified in a search for nearby stars selected by DENIS photometry (Reylé *et al.* 2002). Another one is DENIS-P J210724.7-335733, which was identified as a very nearby star in the DENIS survey (Phan-Bao *et al.* 2001) based on its very red color and large measured proper motion. Four other objects match the stars SSSPM J1148-7458, SSSPM J1358-3938, SSSPM J1530-8146, and SSSPM J1549-3544, all identified by Scholz *et al.* (2004) in a proper motion survey combining the SuperCOSMOS Sky Survey database and positions from the 2MASS and DENIS surveys. We also found a match to the late-type M8 dwarf 2MASSI J1534570-141848, which was observed as part of spectroscopic backup program by Gizis (2002). That star was selected for follow-up observation because of a very red infrared color $J - K_s > 1.0$, indicative of a very low-mass star, so it was not initially identified as a high proper motion object. We find this star to have a very large proper motion $[\mu_{RA}, \mu_{Decl.}] = [-0.931, -0.317]''\text{yr}^{-1}$, and although the star cannot formally be considered a “new discovery”, ours is the first report of a proper motion measurement. Likewise we recovered the star 2MASSI 0417374-080000, also initially identified as a candidate nearby star

($d \simeq 17.4$ pc) from a color-selected subsample of sources from the 2MASS Second Instrumental Release (Cruz *et al.* 2003). We find the star to have a proper motion $[\mu_{RA}, \mu_{Decl.}] = [0.458, 0.041]''\text{yr}^{-1}$. Finally, the esdM7.5 subdwarf 2MASS J12270506-0447207 was also recovered by SUPERBLINK, with a proper motion $[\mu_{RA}, \mu_{Decl.}] = [-0.459, 0.249]''\text{yr}^{-1}$; that star had been recently identified as an ultra-cool subdwarf from a color-selected sample of 2MASS sources (Burgasser, Cruz, & Kirkpatrick 2007).

The location on the sky of all the stars with $0.45''\text{yr}^{-1} < \mu < 2.00''\text{yr}^{-1}$ identified by SUPERBLINK is shown in Figure 3 (top panel). Stars which were listed in the NLTT/LHS catalogs are marked with crosses. Stars discovered in subsequent surveys, as described above, are plotted as triangles.

4. NEW DISCOVERIES

In the end, the list of SUPERBLINK identifications yielded 170 new stars with $0.45''\text{yr}^{-1} < \mu < 2.0''\text{yr}^{-1}$. Their distribution on the sky is shown in Fig.3 (bottom panel). A significant fraction of these new discoveries are located in low Galactic latitude areas, particularly in the general direction of the Galactic center/bulge (around $\alpha=270.0$ $\delta=-30.0$). This reflects the particular ability of the SUPERBLINK software to detect moving stars in fields of high stellar density, areas which were typically avoided in most previous surveys. These areas of low galactic latitude in the southern sky were the very last regions of the sky which remained largely unexplored for faint high proper motion stars. Our survey has now filled this gap.

The complete list of 170 new high proper motion stars is provided in Table 1. All stars from the SUPERBLINK survey are now assigned a designation following the convention introduced in Paper III of this series, which is based on the system initially proposed by Eggen (1979). The prefix “PM” (for Proper Motion) is followed by an alpha-numerical designation which refers to the star’s coordinates. The sequence starts with the letter “I” which indicates that the coordinates are from the ICRS system (all positions are based on 2MASS catalog positions of the infra-red counterparts, which are ICRS resolved). A directional suffix (“N”, “S”, “W”, or “E”) is added to distinguish between stars with similar coordinates. Table 1 gives the Right Ascension and Declination for every star ($\alpha(\text{ICRS})$, $\delta(\text{ICRS})$). The total proper motion of the star (μ) is given in arcsec per year, as well as the component of the proper motion in the directions of R.A. and Decl (μ_α , μ_δ). The temporal baseline (Δt) between the first and second epoch detection is tabulated, from which an estimate of the proper motion error is calculated (μ_{err}).

We searched for counterparts to all the high proper motion stars in the USNO-B1.0 Catalog (Monet *et al.* 2003), from which we extracted optical magnitudes in the blue (B_J) red (R_F) and infrared (I_N) bandpasses. Counterparts were also identified in the 2MASS All-Sky Catalog (Cutri *et al.* 2003), yielding infrared J, H, and K_s magnitudes for most of the stars. All the magnitudes are listed in Table 1. Effective visual magnitudes (V) were then calculated from the photographic magnitudes using the scheme of Lépine, & Shara (2005). The table then lists optical-to-infrared (V-J) colors for all stars with 2MASS counterparts.

A reduced proper motion diagram, plotting $H_V = V + 5 \log \mu + 5$ against $V - J$, is displayed in Figure 4. The top panel shows the stars from earlier catalogs which have been re-identified in our survey; the bottom panel shows the new

³ <http://simbad.u-strasbg.fr/Simbad>

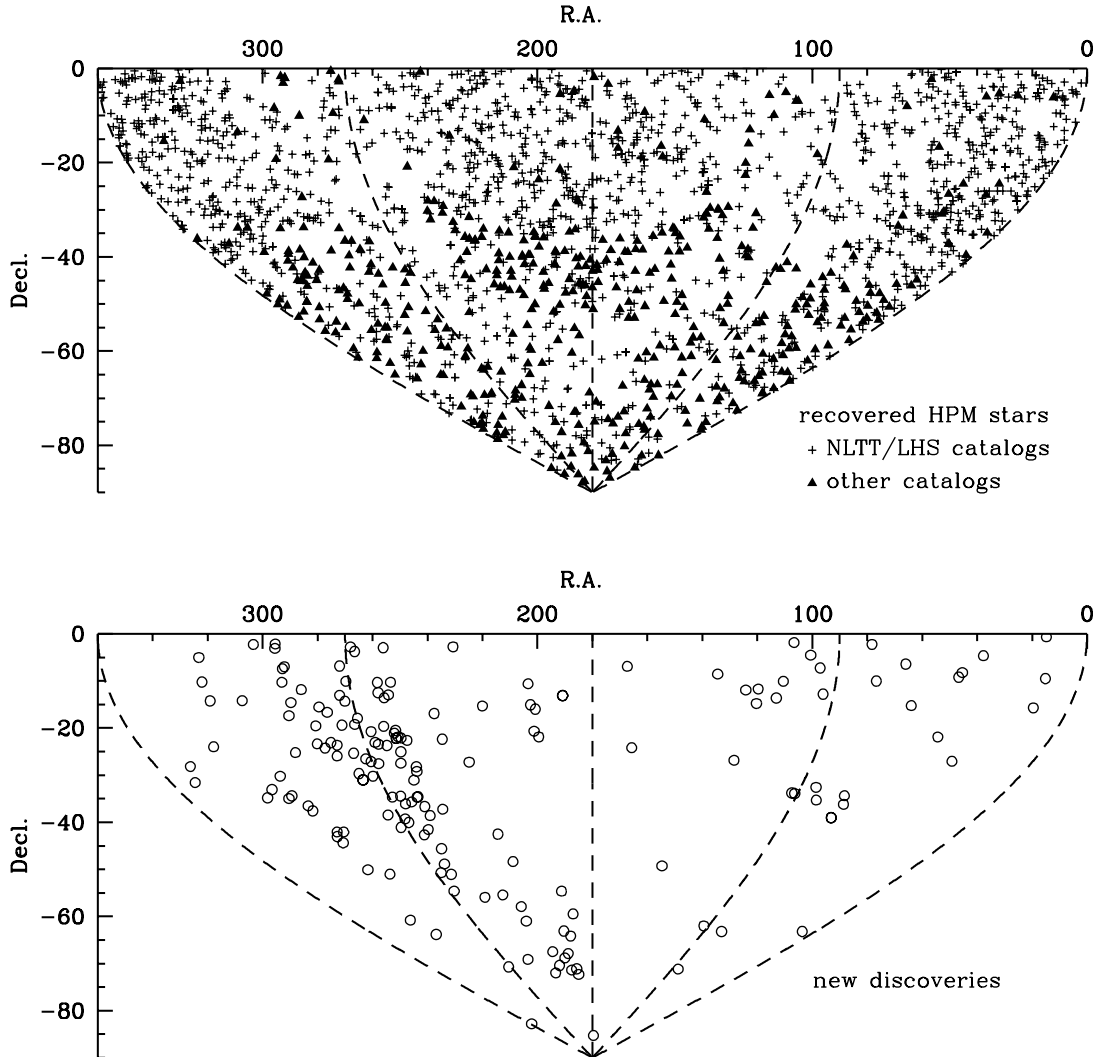


FIG. 3.— Distribution of high proper motion stars identified by SUPERBLINK in southern sky. Top: stars previously reported in the literature, including stars from papers I-III of this series. Crosses mark the stars known at the time of Luyten’s NLTT and LHS catalogs, triangles mark stars discovered in subsequent surveys. Bottom: new high proper motion stars listed in this paper. Many of the new discoveries are in low galactic latitudes and in the general direction of the Galactic center, in fields with high stellar densities.

discoveries. Nearby stars placed in a reduced proper motion diagram occupy one of three distinct loci. Data from our extensive spectroscopic follow-up survey of northern stars with large proper motions (Lépine, Rich, & Shara 2003, 2007) demonstrates that these loci correspond to three distinct spectroscopic classes: low-mass dwarfs (d), low-mass subdwarfs (sd), and white dwarfs (wd). The three classes are arranged in three main “layers” from the upper right to the bottom left of the diagram, respectively, and roughly match the relative locations of the color-magnitude relationships, as one would see them in a color-magnitude diagram. We set the approximate boundaries between the three loci using two straight lines, shown in Fig.4. We use these boundaries to assign each of our stars one of three spectral classes (d/sd/wd). These are essentially predictions of the spectral subclasses, meant to be used only as a guide for future spectroscopic follow-up efforts. Based on our ongoing follow-up spectroscopic survey of over 3,000 stars, this predictor based on the

reduced proper motion is about 90% accurate. The spectral class assignments (d/sd/wd) for the 170 new stars are listed in the last column of Table 1.

5. NOTES ON INDIVIDUAL STARS

5.1. *PM H6230-6905*

With a total proper motion $\mu = 1.594'' \text{ yr}^{-1}$, this star is the fastest of the newly discovered objects. Its location in the reduced proper motion diagram places it within the group of M dwarf from the disk population. However its V magnitude and V-J color yields a photometric distance of ~ 29 parsecs, following the color-magnitude relationship of Lépine (2005). This would indicate a large transverse velocity of $\sim 220 \text{ km s}^{-1}$. Such a large velocity is more usually associated with subdwarfs from the halo. It is very possible that the star is moderately metal-poor ($\log \text{Fe}/\text{H} \approx -0.5$) and also slightly sub-luminous; this will give it a relatively closer photometric distance and smaller transverse velocity. This would be

TABLE 1
RECOVERY RATE BY SUPERBLINK OF KNOWN HIGH PROPER MOTION
STARS FROM VARIOUS CATALOGS¹

Source	southern sky # ²	recovered	missed	recovery rate
Giclas catalog	247	235	12	95.1%
Luyten catalogs	1477	1395	82	94.4%
WT/WC survey	152	139	13	91.4%
Calan-ESO survey	46	42	4	91.3%
APMPM survey	143	118	25	82.5%
LEHPM survey	331	286	45	86.4%
SuperCosmos-RECONS	196	174	22	88.8%
SIPS survey	68	20	48	29.4%

¹ Stars in the southern sky, with proper motions $0.45''\text{yr}^{-1} < \mu < 2.0''\text{yr}^{-1}$, and visual magnitude $V > 10$.

² Total number of objects in the Southern sky. Surveys are not mutually exclusive; stars can be tabulated in several of these lists.

enough to kinematically associate the star with the thick disk population, which would also be consistent with the star being moderately metal poor.

5.2. PM I17189-4131

This star has a total proper motion $\mu = 1.160''\text{yr}^{-1}$. Its very red color ($V - J = 5.51$, $J - K_s = 0.99$) suggests it is a late-type red dwarf, probably of spectral subtype M6. The photometric distance, again following the $[M_V, V - J]$ color-magnitude relationship of Lépine (2005), places it at $d \approx 18$ parsecs. Just like the previous object, the very high proper motion would then indicate a relatively large transverse velocity $v_T \approx 100$ km/s. Spectroscopy is much needed in this case, as it is required to determine whether the star is metal-poor and member of the old disk or thick disk, or whether it could be a kinematically hot member of the thin disk population.

5.3. PM I17595-1755

With a proper motion $\mu = 1.143''\text{yr}^{-1}$, this star has a very large reduced proper motion for an object of that color ($V - J \approx 3.3$). So much so that its location in the reduced proper motion diagram is largely consistent with the halo subdwarf population. Spectral classification would be required to obtain a photometric distance estimate, because color-magnitude relationships for the cool subdwarfs are dependent on metallicity.

5.4. PM I19418-0208

The fourth new star with a proper motion in excess of $1''\text{yr}^{-1}$, this one is remarkably faint ($V \approx 17.5$), and not particularly red ($V - J \approx 2.87$). Its location in the reduced proper motion diagram lies just within the subdwarf range, although there is a chance that the star could be a white dwarf. This is yet another high priority target for spectroscopic follow-up observations.

6. MISSED OBJECTS AND SURVEY COMPLETENESS

In order to assess the completeness of our proper motion survey, we have been compiling hits and misses for stars identified in all the previous surveys. Here we analyze the results for stars with proper motions in the range $0.45''\text{yr}^{-1} < \mu < 2.0''\text{yr}^{-1}$ and excluding the stars which are listed in the TYCHO-2 catalog (i.e. the very bright stars).

To determine the recovery rate and efficiency of the SUPERBLINK software for the southern sky areas, we have compared the complete list of SUPERBLINK detections with the following catalogs and lists of high proper motion objects:

1. The Lowell southern proper motion catalog of Giclas, Burnham, & Thomas (1978)
2. The NLTT catalog of Luyten (1979a).
3. The lists of high proper motion stars identified by Wroblewski & Torres (1997) and Wroblewski & Costa (2001), which we also refer to as the WT/WC survey
4. The Calan-ESO Proper Motion Survey (Ruiz *et al.* 2001).
5. The Liverpool-Edinburgh High Proper Motion Survey (Pokorny, Jones, & Hambly 2003), which we also refer to as the LEHPM survey.
6. The APM proper motion survey (APMPM) of Scholz *et al.* (2000).
7. The SuperCOSMOS-RECONS proper motion survey (Subasavage, *et al.* 2005a,b).
8. The Southern Infrared Proper Motion Survey or SIPS (Deacon, Hambly, & Cooke 2005).

We have carefully cross-correlated all southern sky objects from the catalogs above to identify overlaps and eliminate redundant objects. Many stars were indeed found to be listed in more than one of the catalogs above. As a rule, of course, we only considered stars from these surveys which are not listed in the TYCHO-2 catalog, and with proper motions within the limits of our current data release. Together, the eight catalogs provided a total of 1,962 non-TYCHO stars with proper motion $0.45''\text{yr}^{-1} < \mu < 2.0''\text{yr}^{-1}$.

A cross-correlation with the SUPERBLINK list has yielded matches to 1,730 objects; 232 stars from the catalogs above were not identified by SUPERBLINK. To verify the reality of the missing stars, we have examined Digitized Sky Survey scans centered on the quoted positions of each of the 232 objects. All fields were $10'$ on the side. We were able to confirm the high proper motion status of 210 stars, but failed to identify 22 objects (21 of which were listed only once in the NLTT catalog, and the other one mentioned only once in the LEHPM survey); we must assume these stars to be either spurious, or to have such large errors on their reported positions ($> 5'$) that the stars are effectively “lost”. In the end, we find that our SUPERBLINK survey failed to recover 210 genuine high proper motion stars out of 1,940 genuine objects, suggesting an overall recovery rate of 89.2%.

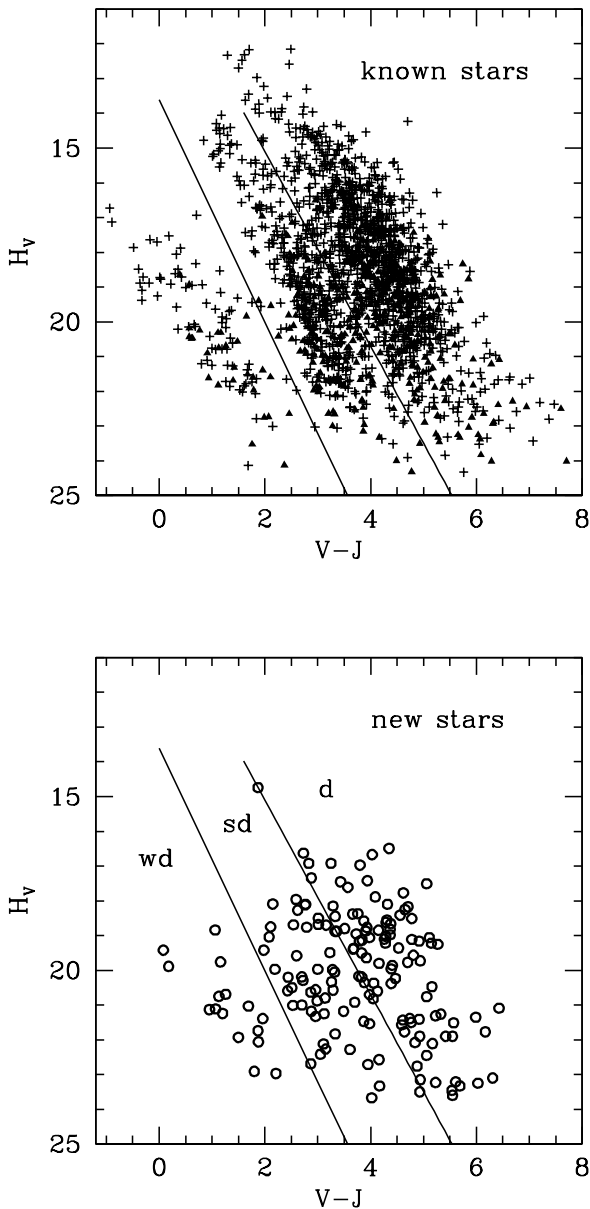


FIG. 4.— Reduced proper motion diagrams of the stars identified by SUPERBLINK. Top: previously known HPM stars. Labels have the same meaning as in Fig.3, with crosses denoting stars from the NLTT/LHS catalogs, and triangles stars that were discovered since the Luyten surveys. Bottom: new high proper motion stars discovered with SUPERBLINK. The location on the diagram is used to separate the stars in one of three classes: white dwarfs (wd), subdwarfs (sd), and dwarfs (d), which occupy distinct loci – most apparent in the top panel. The subdwarfs are typically associated with the Galactic halo, and the dwarfs with the Galactic disk.

We compile in Table 2 the number of hits and misses from each of the older surveys, and calculate the effective rate of recovery by SUPERBLINK. A disproportionate number of misses are from the SIPS survey, from which SUPERBLINK recovered only 20 of the 68 stars. The SIPS survey was based on a comparison of infra-red images, and was thus particularly sensitive to extremely red objects, particularly brown dwarfs; objects like these often do not show up on the optical images

of the Digitized Sky Surveys. Because SUPERBLINK always used at least one of the blue and red photographic plates, these objects could not possibly have been detected. If we exclude misses from the SIPS catalog, which could not possibly have been detected anyway, then we find an overall recovery rate of 91.4% for SUPERBLINK.

Figure 5 shows the color-magnitude distribution of the stars recovered and missed by SUPERBLINK. The top panel shows the recovered objects, and the middle panels the stars missed by the code. SUPERBLINK has a recovery rate exceeding 90% for all stars with V magnitude brighter than 19.0. We take this to be the magnitude limit of our survey, and denote it with a dashed line in Fig.5. Stars with $V < 19$ that were missed by SUPERBLINK have a distribution of magnitudes and colors which matches the distribution from recovered objects. This indicates that most of the misses are not related to any magnitude or color selection effects. Most of the misses are located at high Galactic latitudes ($|b| > 20$), but this is probably just because earlier surveys did not have a good coverage of the low Galactic latitudes.

Rather, objects are probably missed when SUPERBLINK fails to properly process specific pairs of photographic plate scans. The software uses $17' \times 17'$, which can be improperly processed for a variety of reasons. One is the presence of an extremely bright ($V \lesssim 5$) saturated star in the field which makes it difficult to properly align the first and second epoch image. Problems also often arise in fields which are extremely sparse, because the software requires a minimum number of background sources in the $17' \times 17'$ subfields to again properly align the first and second epoch images. Additional problems arise when images from each of the two epochs are of very different quality, particularly if there are significant differences in the seeing or magnitude depth. All these possible problems interfere with the detection of high proper motion stars in seemingly randomly distributed fields in the southern sky, which would yield misses with no obvious trend in color or magnitude.

7. CONCLUSIONS

Our hunt for stars with very large proper motions detected in the Digitized Sky Surveys is now coming to an close. We are confident that the vast majority of H-burning stars with proper motions $0.45'' \text{ yr}^{-1} < \mu < 2.0'' \text{ yr}^{-1}$ have now been identified over the entire sky, which completes the efforts undertaken by W. J. Luyten over 60 years ago. The 170 new stars presented in this paper most likely represent the very last, large contingent of new stars with very large proper motions. We find that the SUPERBLINK survey was particularly useful in locating missing high proper motion stars in dense fields at low Galactic latitudes, although it is likely that a few stars remain to be identified in the densest Milky Way fields.

The reduced proper motion diagram shows that the new stars are a mix of nearby disk dwarfs, halo subdwarfs, and white dwarfs. We tentatively assign each of the new stars to one of the three main classes. It is however clear from the few examples in §5 that spectroscopic follow-up is required to ascertain the status of several of the stars. Likewise, many of the previously known high proper motion stars in the southern sky still have no formal spectral classification, and should be considered high priority targets.

Lists of southern stars with high proper motions are unfortunately still scattered throughout the astronomical literature, in no less than 8 separate publications. The upcoming LSPM-south catalog (Lépine *et al.*, in preparation) will remedy this

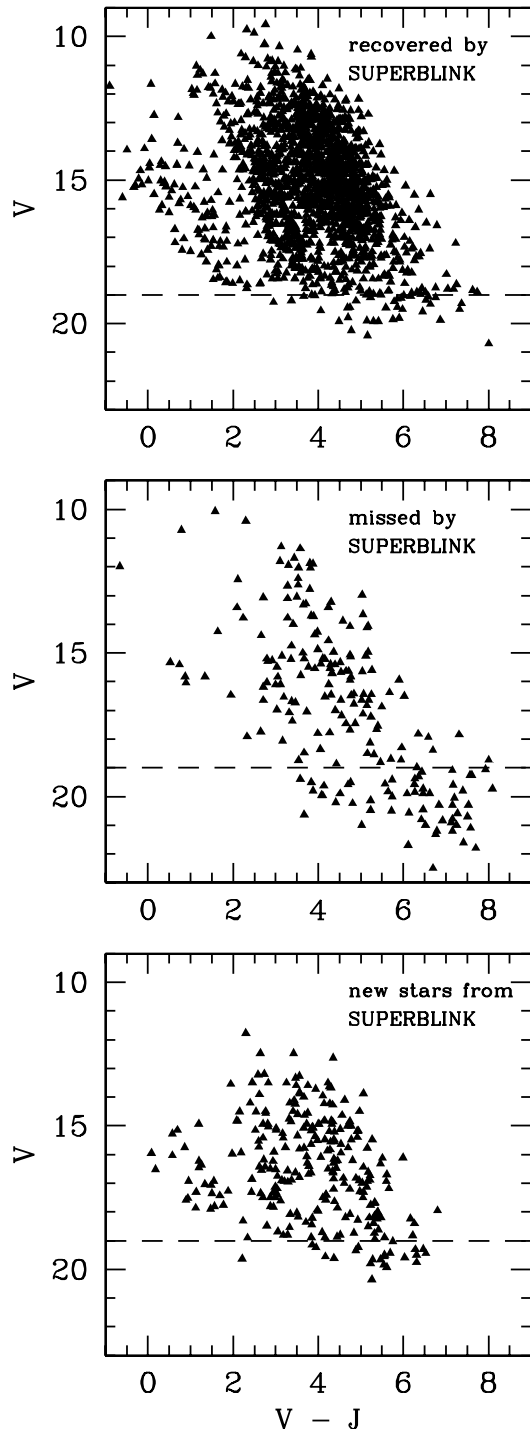


FIG. 5.— Distribution of apparent visual magnitudes (V) and optical-to-infrared color ($V-J$) of high proper motion stars ($0.45''\text{yr}^{-1} < \mu < 2.0''\text{yr}^{-1}$) identified in the entire southern celestial hemisphere (excluding bright TYCHO-2 catalog objects). Top panel: known stars re-identified by SUPERBLINK (“hits”). Center: known stars that were not recovered by SUPERBLINK (“misses”). Bottom: new stars identified with SUPERBLINK, and listed in Table 2 of this paper. The recovery rate by SUPERBLINK of previously known stars is larger than 90% for visual magnitudes $V < 19$ (dashed line).

problem by combining all the stars in a single catalog. We now have all-sky lists of SUPERBLINK detections down to proper motions of $0.15''\text{yr}^{-1}$. What needs to be done now is the independent validation of the high proper motion stars reported in other surveys but missed by SUPERBLINK.

In any case, census of stars with very large proper motions $\mu > 0.45''\text{yr}^{-1}$ is now largely complete down to magnitude $V = 19.0$. The census of objects with very large proper motion is however still incomplete at fainter magnitudes. Objects that await discovery most likely include a number of old white dwarfs and ultra-cool dwarfs and subdwarfs, all too faint to be detected in the Digitized Sky Surveys. It is also likely that brighter HPM stars are still hiding in very dense field, or at short angular separations from very bright stars, since their images would have been engulfed within the photographically saturated patches of their very bright line-of-sight companions. However, we suspected that the bulk of the still missing high proper motion object most probably consist of all types of brown dwarfs and other extremely red and low-luminosity objects. Their discovery will require deep, multi-epoch surveys, preferably conducted at infra-red wavelengths.

Acknowledgments

This research program was supported by the National Science Foundation through grant AST-0607757, held at the American Museum of Natural History. SL also gratefully acknowledge support from Hilary Lipsitz.

This work has been made possible through the use of the Digitized Sky Surveys. The Digitized Sky Surveys were produced at the Space Telescope Science Institute under U.S. Government grant NAG W-2166. The images of these surveys are based on photographic data obtained using the Oschin Schmidt Telescope on Palomar Mountain and the UK Schmidt Telescope. The plates were processed into the present compressed digital form with the permission of these institutions. The National Geographic Society - Palomar Observatory Sky Atlas (POSS-I) was made by the California Institute of Technology with grants from the National Geographic Society. The Second Palomar Observatory Sky Survey (POSS-II) was made by the California Institute of Technology with funds from the National Science Foundation, the National Geographic Society, the Sloan Foundation, the Samuel Oschin Foundation, and the Eastman Kodak Corporation. The Oschin Schmidt Telescope is operated by the California Institute of Technology and Palomar Observatory. The UK Schmidt Telescope was operated by the Royal Observatory Edinburgh, with funding from the UK Science and Engineering Research Council (later the UK Particle Physics and Astronomy Research Council), until 1988 June, and thereafter by the Anglo-Australian Observatory. The blue plates of the southern Sky Atlas and its Equatorial Extension (together known as the SERC-J), as well as the Equatorial Red (ER), and the Second Epoch [red] Survey (SES) were all taken with the UK Schmidt.

This publication makes use of data products from the Two Micron All Sky Survey, which is a joint project of the University of Massachusetts and the Infrared Processing and Analysis Center/California Institute of Technology, funded by the National Aeronautics and Space Administration and the National Science Foundation.

The data mining required for this work has been made possible with the use of the SIMBAD astronomical database and VIZIER astronomical catalogs service, both maintained and

operated by the Centre de Données Astronomiques de Strasbourg⁴.

This research used the facilities of the Canadian Astronomy

⁴ <http://cdsweb.u-strasbg.fr/>

⁵ <http://www4.cadc-ccda.hia-ihp.nrc-cnrc.gc.ca/cadc/>

Data Centre⁵ operated by the National Research Council of Canada with the support of the Canadian Space Agency.

REFERENCES

- Bakos, G. A., Sahu, K. C., & Nemeth, P. 2002, *ApJS*, 141, 187
 Burgasser, A. J., Cruz, K. L., & Kirkpatrick, J. D. 2007, *ApJ*, 657, 494
 Cruz, K. L. 2003, *et al.* 2003, *AJ*, 126, 2421
 Cutri, R. M., *et al.* 2003, The 2MASS All-Sky Catalog of Point Sources
 University of Massachusetts and Infrared Processing and Analysis Center
 (IPAC/California Institute of Technology – *CDS-ViZier catalog number II/246*)
 Dawson, P. C. 1986, *ApJ*, 311, 984
 Deacon N.R., Hambly N.C., & Cooke J.A. 2005, *A&A*, 435, 363
 Eggen, O. J. 1979, *ApJS*, 39, 89
 Giclas, H.L., Burnham, R., & Thomas, N.G. 1971, Lowell proper motion
 survey Northern Hemisphere, Flagstaff, Arizona: Lowell Observatory.
 Giclas, H.L., Burnham, R., & Thomas, N.G. 1978, Lowell Proper Motion
 Survey - Southern Hemisphere Catalog, Bulletin. Lowell Observatory V.8,
 P.89
 Gizis, J. E. 2002, *ApJ*, 575, 484
 Gould, A., Salim, S. 2003, *ApJ*, 582, 1001
 Lépine, S., Shara, M. M., & Rich, R. M. 2002, *AJ*, 124, 1190
 Lépine, S., Rich, R. M., & Shara, M. M. 2003, *AJ*, 125, 1598
 Lépine, S., Shara, M. M., & Rich, R. M. 2003, *AJ*, 126, 921
 Lépine, S., Rich, R. M., & Shara, M. M. 2007, *ApJ*, 669, 1235
 Lépine, S., & Shara, M. M. 2005, *AJ*, 126, 921
 Lépine, S. 2005, *AJ*, 130, 1247
 Levine, S. E. 2005, *AJ*, 130, 319
 Luyten W. J. 1979a, LHS Catalogue: a catalogue of stars with proper
 motions exceeding 0.5" annually, University of Minnesota, Minneapolis
 (*CDS-ViZier catalog number I/87B*)
 Luyten W. J. 1979b, New Luyten Catalogue of stars with proper motions
 larger than two tenths of an arcsecond (NLTT), University of Minnesota,
 Minneapolis (*CDS-ViZier catalog number I/98A*)
 McCook, G. P., & Sion, E. M. 1999, *ApJS*, 121, 1
 Monet, D. G., *et al.* 2003, *AJ*, 125, 984, (The USNO-B1 catalog –
CDS-ViZier catalog number I/284)
 Oppenheimer, B. R., *et al.* 2001, *Science*, 292, 698
 Phan-Bao N., *et al.* 2001, *A&A*, 380, 590
 Pokorny, R. S., Jones, H. R. A., & Hambly, N. C. 2003, *A&A*, 397, 584
 Reylé, C., *et al.* 2002, *A&A*, 390, 491
 Ruiz, M. T., Leggett, S. K., & Allard, F. 1997, *ApJ*, 491, L107
 Ruiz, M. T., Wischnjewsky, M., Rojo, P. M., & Gonzalez, L. E. 2001, *ApJS*,
 133, 119
 Salim, S., & Gould, A. 2003, *ApJ*, 582, 1011
 Scholz, R.-D., Irwin, M., Ibata, R., Jahreiss, H., & Malkov, O. Yu. 2000,
A&A, 353, 958
 Scholz, R.-D., Lehmann, I., Matute, I., & Zinnecker, H. 2004, *A&A*, 425,
 519
 Subasavage, J. P., *et al.* 2005a, *AJ*, 129, 413
 Subasavage, J. P., *et al.* 2005b, *AJ*, 130, 1658
 Wroblewski, H., & Torres, A. 1997, *A&AS*, 122, 447
 Wroblewski, H., & Costa, E. 2001, *A&A*, 367, 725

APPENDIX

FINDER CHARTS

Finder charts of high proper motion stars are generated as a by-product of the SUPERBLINK software. We present here finder charts for all the new, high proper motion stars presented in this paper and listed in Table 1. Each charts consist in a pair of images showing the local field at two different epochs. The name of the star is indicated in the center just below the chart, and corresponds to the name given in Table 1. To the left is the POSS-I field, with the epoch of the field noted in the lower left corner. To the right is the modified POSS-II field which has been shifted, rotated, and degraded in such a way that it matches the quality and aspect of the POSS-I image. The epoch of the POSS-II field is noted on the lower right corner. High proper motion stars are identified with circles centered on their positions at the epoch on the plate.

The charts are oriented in the local X-Y coordinate system of the POSS-I image; the POSS-II image has been remapped on the POSS-I grid. The specific orientation of each field is specified by a north-east (N-E) compass, drawn on the first epoch panel. Each segment of the compass is 1 arcminute in length, which provides a sense of scale. Most of the charts are $4.25' \times 4.25'$ on the side, but a few are $2.5' \times 2.5'$ on the side. Those are easily distinguished by the size of the N-E compass.

Sometimes a part of the field is missing: this is an artifact of the code. SUPERBLINK works on $17' \times 17'$ DSS subfields. If a high proper motion star is identified near the edge of that subfield, the output chart appears truncated.

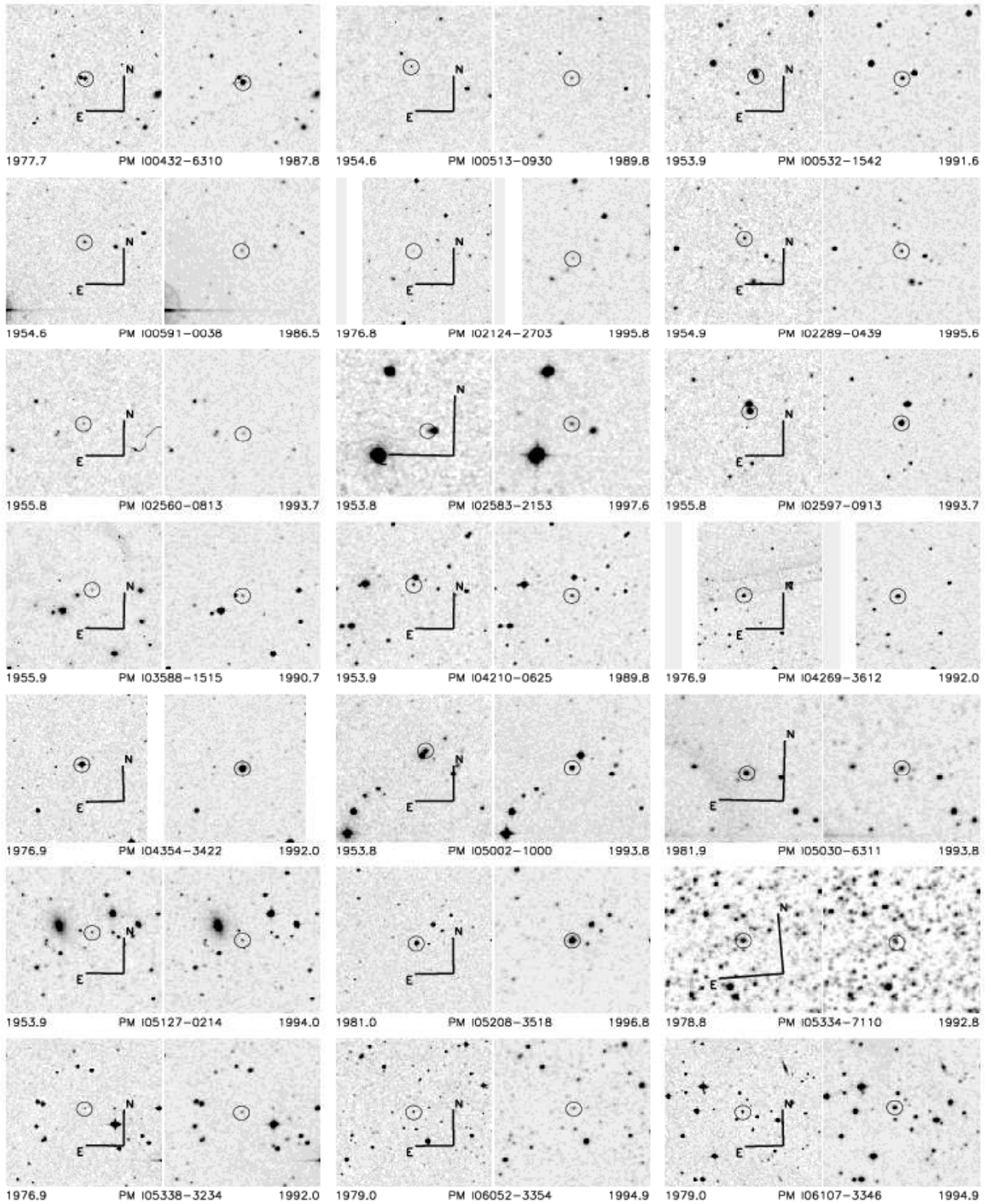


FIG. 6.— Finding charts for the new high proper motion stars discovered with SUPERBLINK, as listed in Table 1.

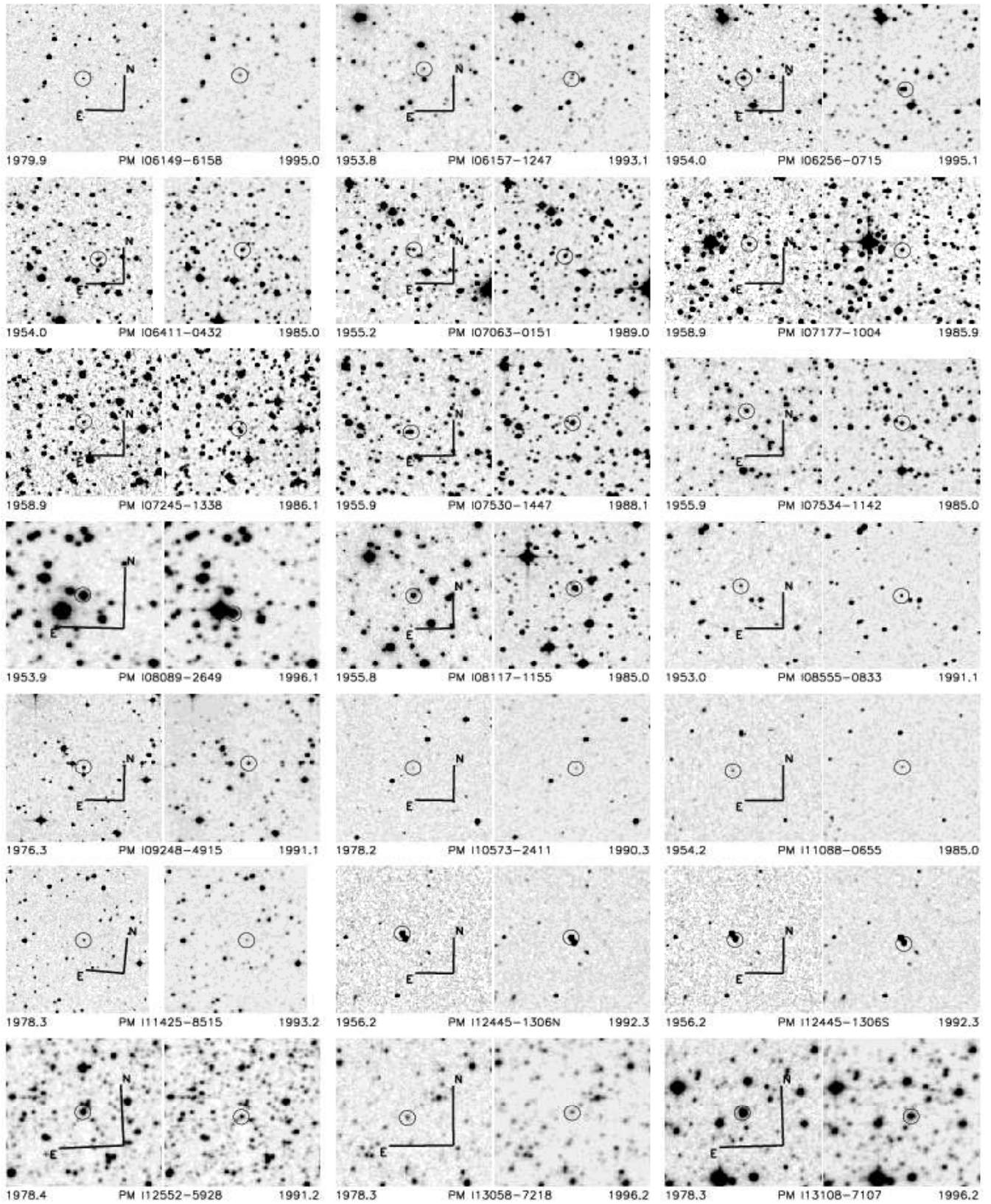


FIG. 7.— Finding charts for the new high proper motion stars discovered with SUPERBLINK (continued).

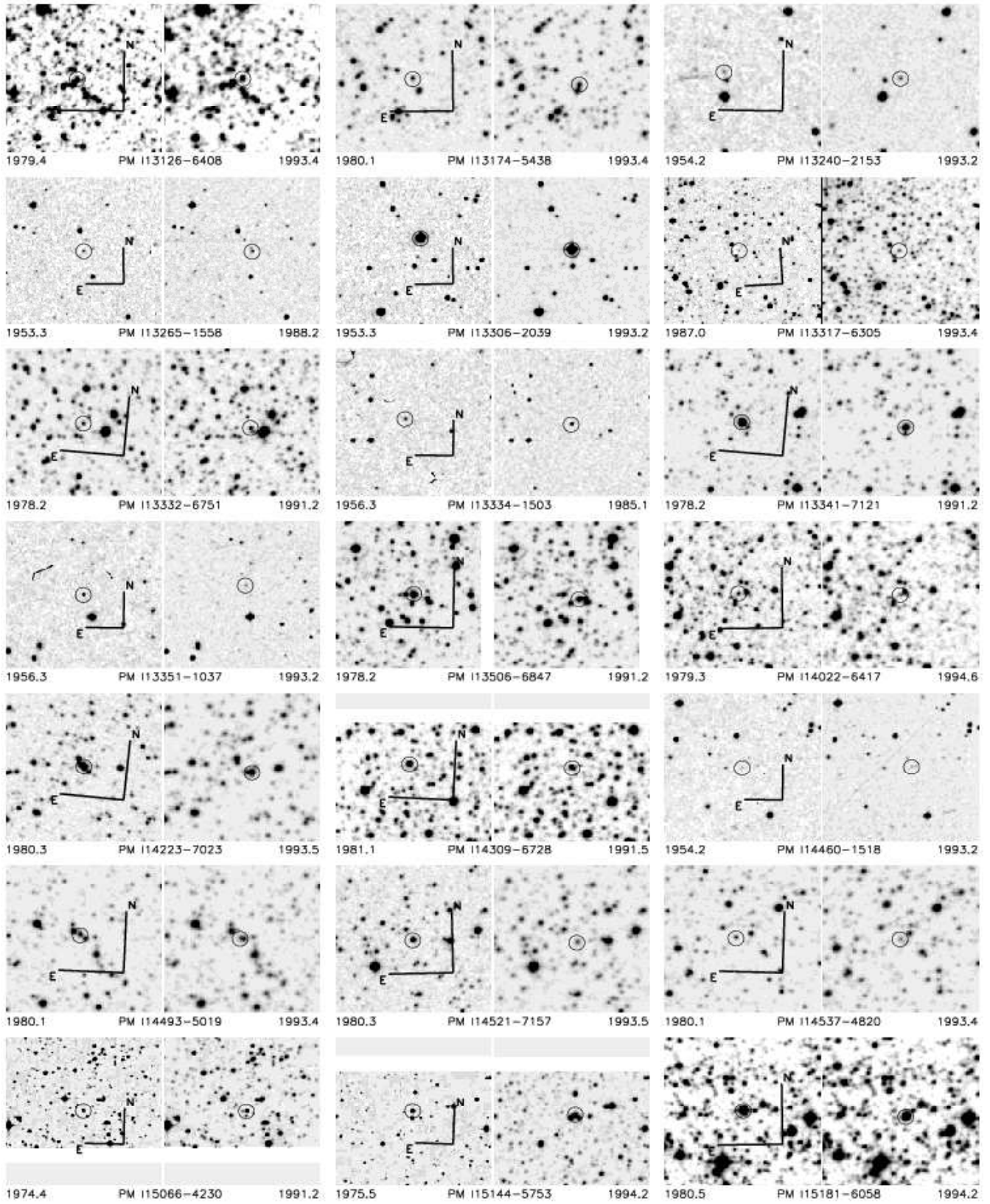


FIG. 8.— Finding charts for the new high proper motion stars discovered with SUPERBLINK (continued).

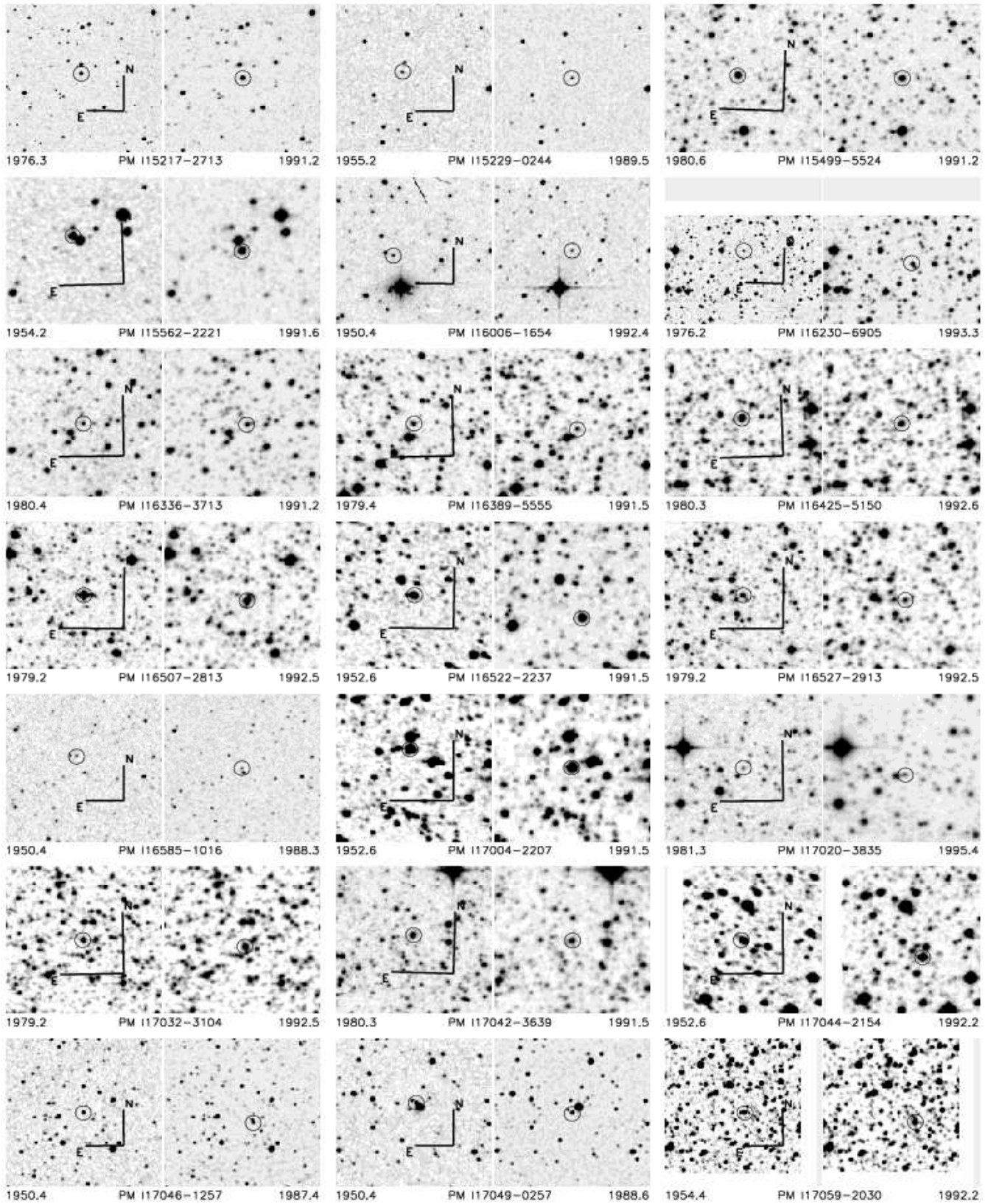


FIG. 9.— Finding charts for the new high proper motion stars discovered with SUPERBLINK (continued).

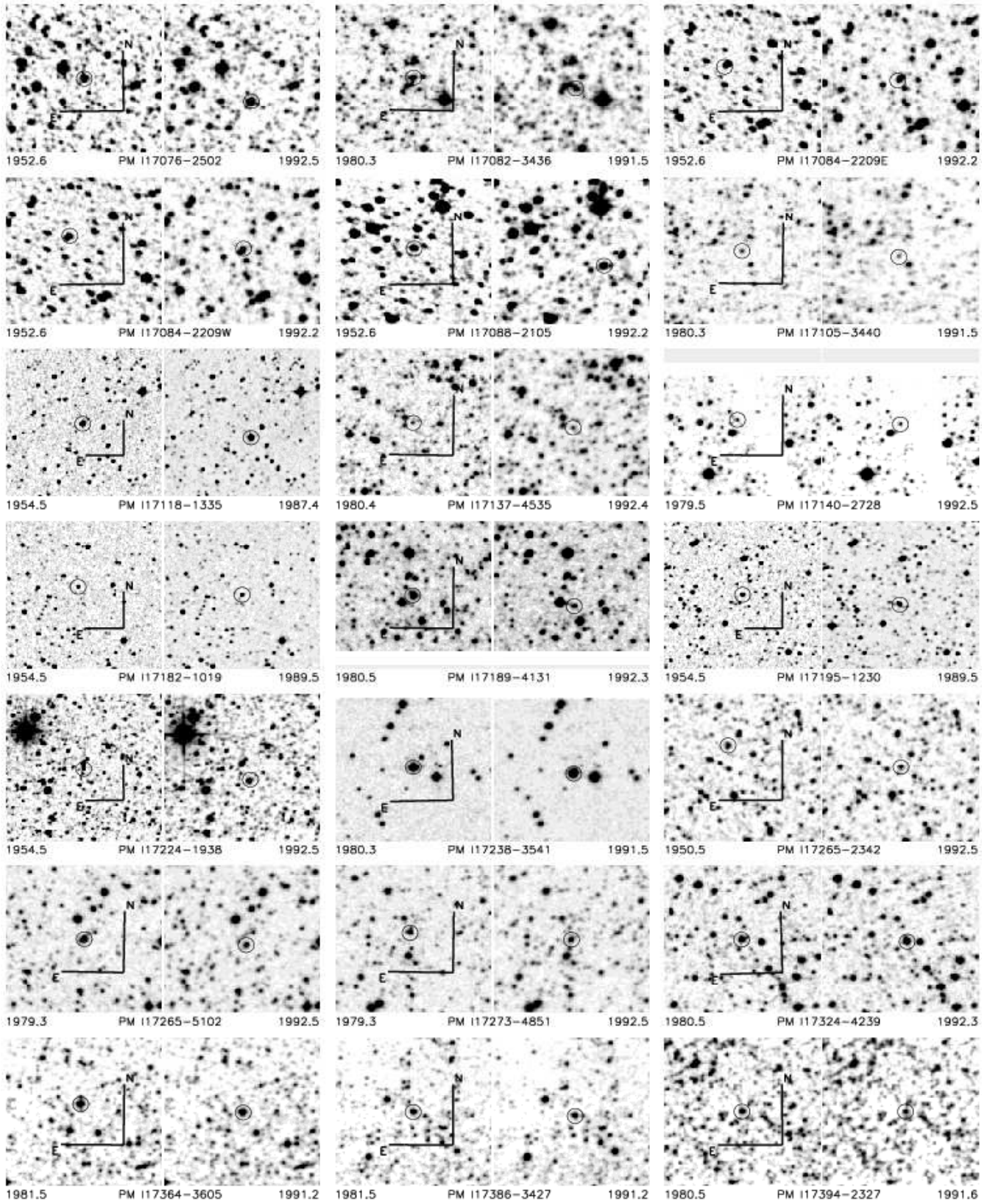


FIG. 10.— Finding charts for the new high proper motion stars discovered with SUPERBLINK (continued).

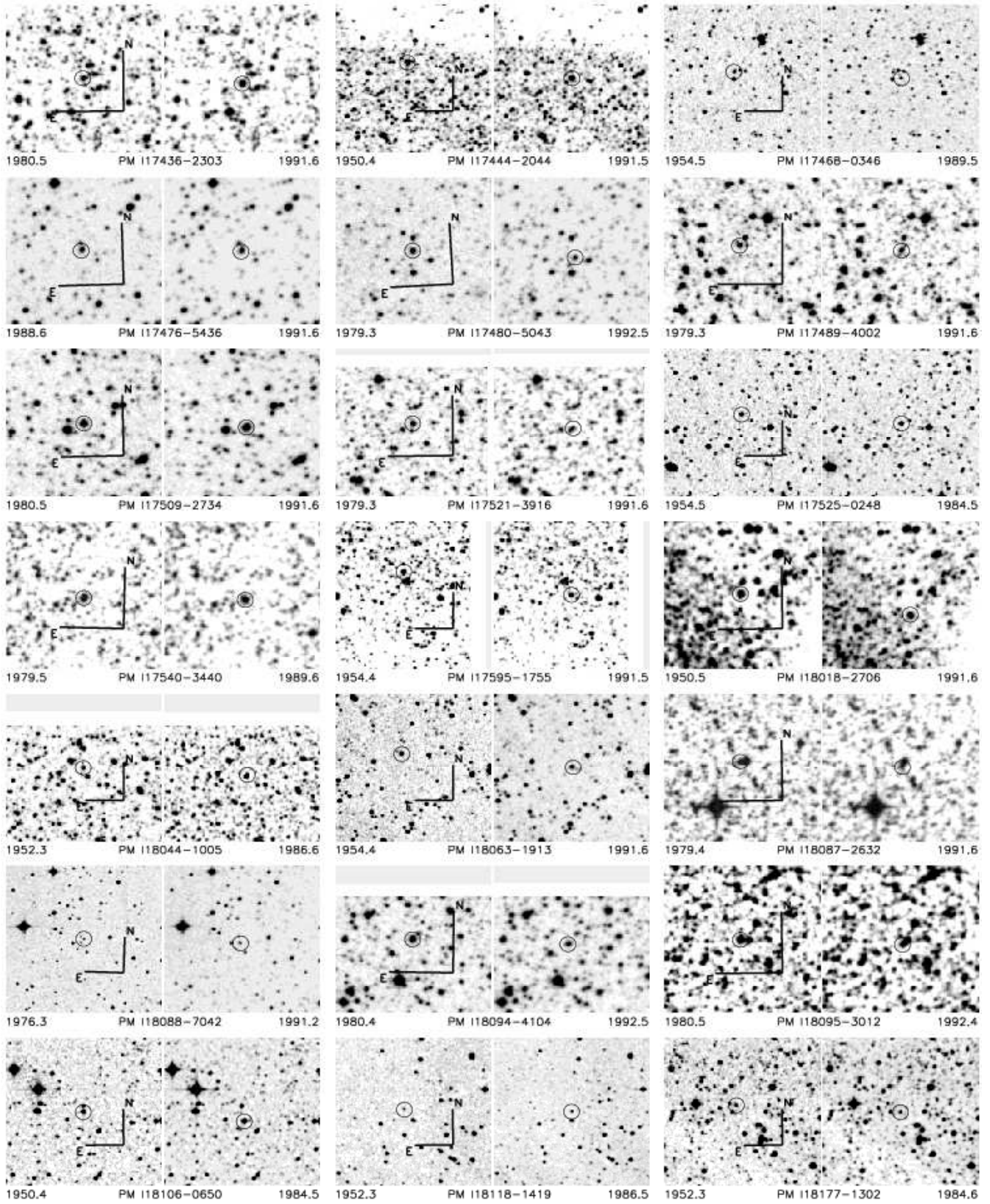


FIG. 11.— Finding charts for the new high proper motion stars discovered with SUPERBLINK (continued).

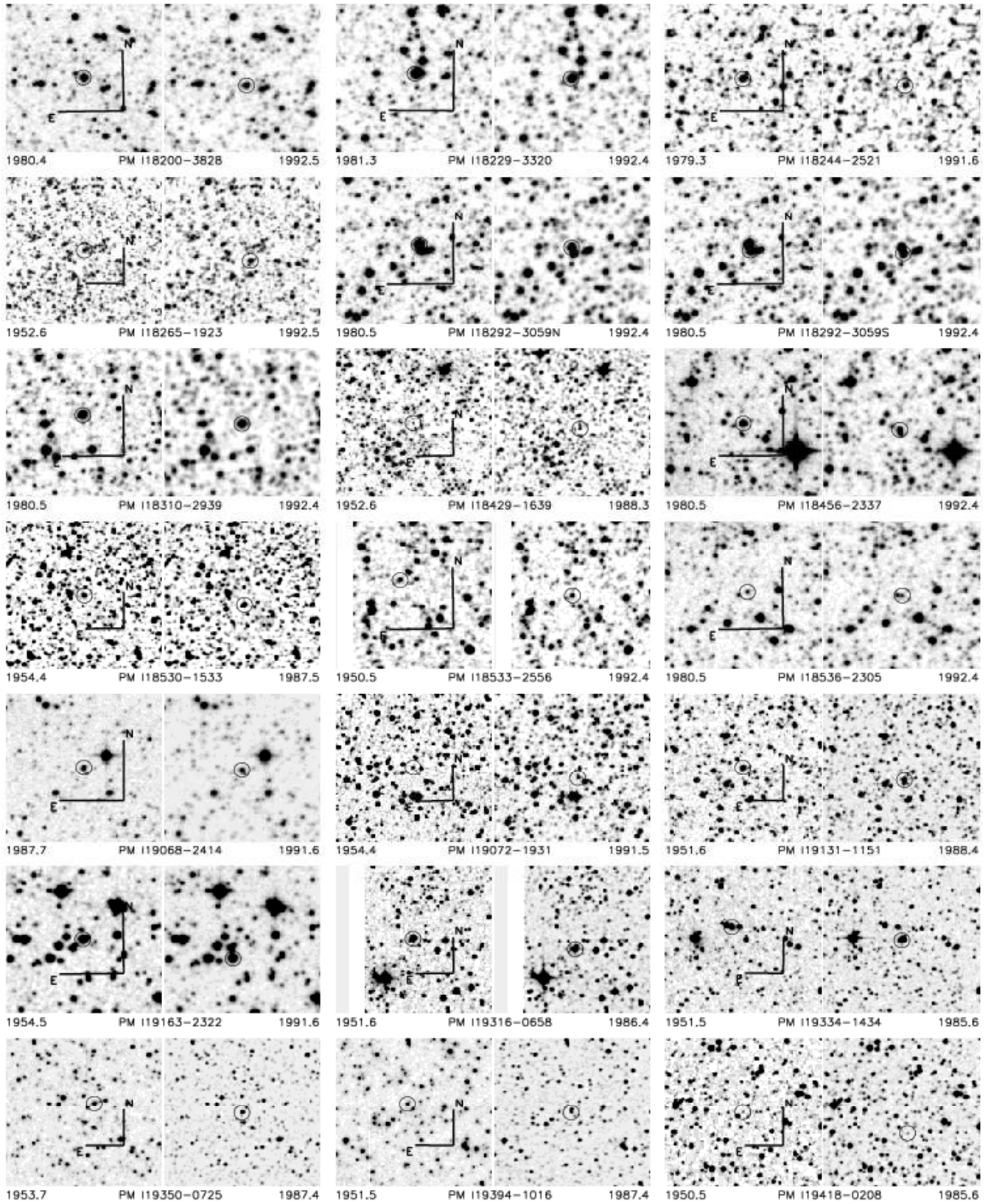


FIG. 12.— Finding charts for the new high proper motion stars discovered with SUPERBLINK (continued).

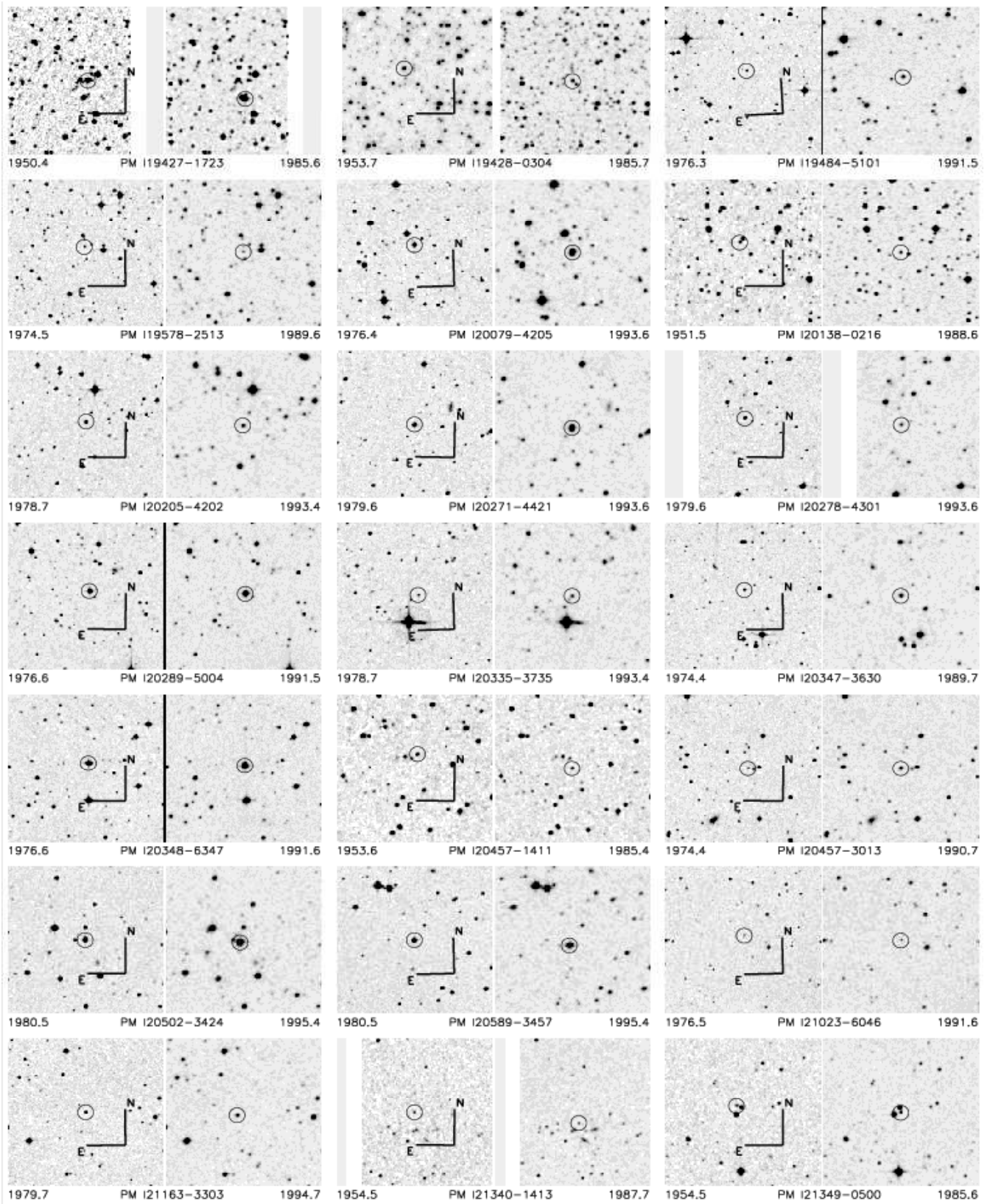


FIG. 13.— Finding charts for the new high proper motion stars discovered with SUPERBLINK (continued).

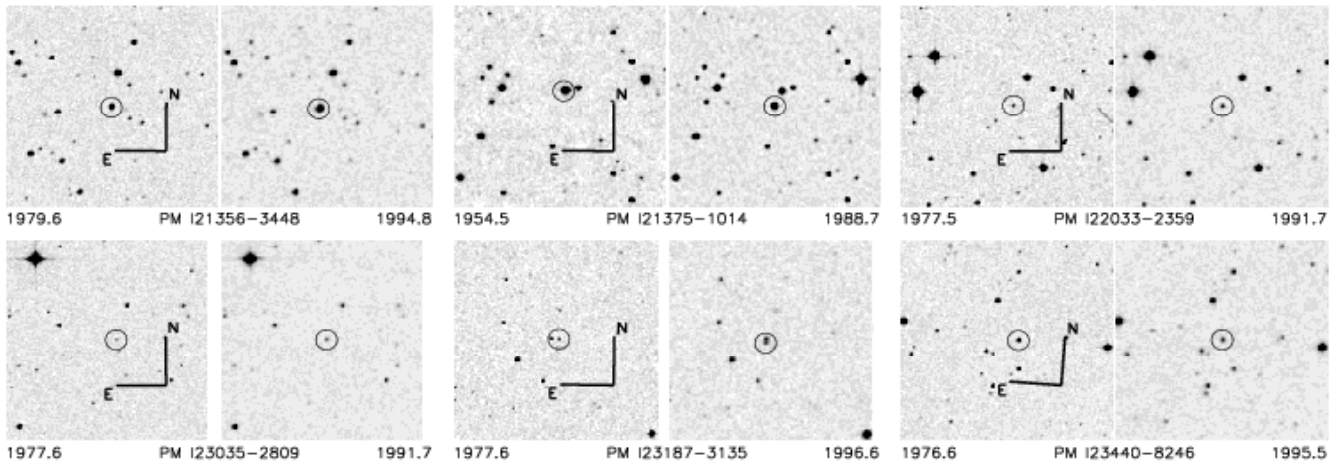


FIG. 14.— Finding charts for the new high proper motion stars discovered with SUPERBLINK (continued).

TABLE 2
NEW HIGH PROPER MOTION STARS.

Star	α (ICRS)	δ (ICRS)	μ ($''$ yr $^{-1}$)	μ_α ($''$ yr $^{-1}$)	μ_δ ($''$ yr $^{-1}$)	Δr^a (yr)	μ_{err}^b ($''$ yr $^{-1}$)	B_J^c	R_F	I_N	J^d	K	H	V	$V-J$	class
PM I00432-6310	10.814372	-63.178169	0.699	0.264	-0.647	10.0	0.040	99.8	14.1	12.9	12.74	12.22	12.06	14.82	2.08	sd
PM I00513-0930	12.846331	-9.501763	0.571	-0.096	-0.563	35.1	0.011	20.1	18.9	17.1	15.38	14.92	14.74	19.55	4.17	sd
PM I00532-1542	13.324378	-15.710962	0.527	0.517	-0.101	37.7	0.011	18.2	15.5	14.4	13.67	13.10	12.90	16.96	3.29	sd
PM I00591-0038	14.794205	-0.647302	0.461	0.084	-0.453	31.9	0.013	19.4	18.1	17.4	15.69	15.59	15.19	18.80	3.11	sd
PM I02124-2703	33.124096	-27.060802	0.697	-0.043	-0.696	18.9	0.021	20.0	19.0	99.8	99.99	99.99	99.99	19.54	99.99	?
PM I02289-0439	37.230431	-4.662395	0.546	0.054	-0.543	40.7	0.010	20.4	17.1	15.4	14.72	14.23	13.93	18.88	4.16	sd
PM I02560-0813	44.009895	-8.220679	0.453	-0.044	-0.451	37.9	0.011	20.8	18.9	16.2	14.32	13.75	13.39	19.93	5.61	d
PM I02583-2153	44.582863	-21.890055	0.539	0.508	0.180	43.7	0.009	20.1	19.0	15.1	13.56	13.06	12.71	19.59	6.03	d
PM I02597-0913	44.949638	-9.219873	0.604	0.296	-0.527	37.8	0.011	16.8	13.3	12.3	10.93	10.42	10.14	15.19	4.26	d
PM I03588-1515	59.710186	-15.252027	0.484	0.375	-0.306	34.7	0.012	21.0	18.4	15.9	14.57	14.24	13.84	19.80	5.23	d
PM I04210-0625	65.254318	-6.429371	0.532	0.019	-0.532	35.9	0.011	21.9	17.4	16.1	14.29	13.81	13.45	19.83	5.54	d
PM I04269-3612	66.744637	-36.212078	0.471	0.469	-0.038	15.0	0.027	99.8	15.1	12.6	11.39	10.86	10.54	16.20	4.81	d
PM I04354-3422	68.871231	-34.368519	0.495	-0.164	-0.467	15.0	0.027	99.8	12.4	10.7	9.70	9.15	8.88	13.50	3.80	d
PM I05002-1000	75.056885	-10.016049	0.901	0.491	-0.755	39.9	0.010	16.8	13.8	13.2	12.72	12.28	12.08	15.42	2.70	sd
PM I05030-6311	75.765450	-63.185085	0.528	0.305	0.431	11.9	0.034	19.4	16.2	15.1	13.95	13.44	13.25	17.93	3.98	sd
PM I05127-0214	78.186485	-2.237835	0.482	0.332	-0.350	40.0	0.010	20.4	18.1	16.3	14.46	13.98	13.71	19.34	4.88	d
PM I05208-3518	80.218033	-35.304283	0.466	0.351	0.306	15.7	0.025	15.4	12.6	11.8	10.68	10.10	9.83	14.11	3.43	d
PM I05334-7110	83.369072	-71.172531	0.489	0.478	-0.104	14.0	0.029	16.8	16.2	14.6	13.52	12.99	12.76	16.52	3.00	sd
PM I05338-3234	83.465843	-32.573948	0.481	0.122	-0.465	15.0	0.027	20.1	18.9	18.6	99.99	99.99	99.99	19.55	99.99	?
PM I06052-3354	91.304489	-33.904339	0.454	-0.189	0.413	15.9	0.025	19.4	17.7	14.7	13.20	12.61	12.25	18.62	5.42	d
PM I06107-3346	92.687683	-33.772923	0.766	0.601	0.475	15.9	0.025	18.1	15.9	13.6	11.52	10.94	10.66	17.09	5.57	d
PM I06149-6158	93.740448	-61.982430	0.479	0.156	0.453	15.0	0.027	99.8	17.0	14.7	13.33	12.89	12.53	18.10	4.77	d
PM I06157-1247	93.931671	-12.789595	0.618	0.452	-0.421	39.2	0.010	20.7	18.2	16.6	14.62	14.13	13.68	19.55	4.93	sd
PM I06256-0715	96.414886	-7.258792	0.478	-0.106	-0.466	41.1	0.010	16.7	14.8	13.0	11.55	10.99	10.67	15.83	4.28	d
PM I06411-0432	100.299698	-4.536717	0.906	0.751	0.506	31.0	0.013	18.1	16.3	16.0	15.39	15.35	15.24	17.27	1.88	wd
PM I07063-0151	106.585503	-1.859489	0.469	0.355	-0.307	33.8	0.012	20.2	17.0	14.9	13.89	13.41	13.14	18.73	4.84	d
PM I07177-1004	109.427681	-10.080668	0.510	0.314	-0.402	27.0	0.015	19.2	17.1	99.8	12.06	11.48	11.15	18.23	6.17	d
PM I07245-1338	111.145668	-13.641150	0.488	0.158	-0.462	27.2	0.015	18.0	16.5	16.8	16.18	16.15	15.61	17.31	1.13	wd
PM I07530-1447	118.274628	-14.786615	0.534	-0.199	0.496	32.2	0.012	17.1	15.2	13.2	11.82	11.28	11.04	16.23	4.41	d
PM I07534-1142	118.358902	-11.700098	0.753	0.209	-0.723	29.0	0.014	18.1	15.9	15.2	13.22	12.74	12.54	17.09	3.87	sd
PM I08089-2649	122.229820	-26.827749	0.485	0.191	-0.446	42.1	0.010	16.7	14.2	12.7	11.18	10.68	10.43	15.55	4.37	d
PM I08117-1155	122.937828	-11.918666	0.466	-0.150	0.441	29.1	0.014	16.4	14.4	13.6	11.11	10.60	10.30	15.48	4.37	d
PM I08555-0833	133.894638	-8.562494	0.467	-0.075	-0.461	38.1	0.010	18.5	17.5	17.2	16.08	15.84	15.28	18.04	1.96	wd
PM I09248-4915	141.204376	-49.258228	0.910	-0.694	0.588	14.8	0.027	17.0	15.8	15.8	15.25	14.92	14.80	16.45	1.20	wd
PM I10573-2411	164.337021	-24.184950	0.605	-0.604	-0.032	12.1	0.033	20.3	18.4	15.7	13.74	13.21	12.86	19.43	5.69	d
PM I11088-0655	167.221176	-6.924221	0.641	-0.596	0.237	30.8	0.013	20.1	18.4	17.8	99.99	99.99	99.99	19.32	99.99	?
PM I11425-8515	175.638351	-85.262344	0.473	-0.469	0.060	14.9	0.027	18.4	18.5	17.9	99.99	99.99	99.99	18.45	99.99	?
PM I12445-1306S	191.132065	-13.107369	0.511	-0.476	-0.186	36.1	0.011	16.2	13.9	12.5	12.13	11.54	11.34	15.14	3.01	sd
PM I12445-1306N	191.133575	-13.104939	0.511	-0.476	-0.186	36.1	0.011	15.8	13.1	12.1	11.79	11.25	11.03	14.56	2.77	sd
PM I12552-5928	193.800598	-59.471436	0.503	0.137	-0.484	12.8	0.031	19.1	15.8	13.9	11.15	10.58	10.21	17.58	6.43	d
PM I13058-7218	196.465515	-72.302284	0.456	-0.335	0.310	17.8	0.022	17.9	16.7	16.6	14.70	14.24	14.07	17.21	2.51	sd
PM I13108-7107	197.716721	-71.119659	0.561	-0.510	-0.234	17.8	0.022	15.8	13.8	12.0	10.59	10.06	9.72	14.88	4.29	d
PM I13126-6408	198.169327	-64.142029	0.487	-0.485	0.041	14.0	0.029	99.8	15.3	15.1	14.00	13.58	13.30	15.98	1.98	sd
PM I13174-5438	199.364120	-54.635632	0.732	-0.569	-0.461	13.2	0.030	17.1	15.5	15.8	15.10	14.76	14.65	16.36	1.26	wd
PM I13240-2153	201.010391	-21.884447	0.483	-0.455	-0.162	38.9	0.010	20.4	19.1	18.7	99.99	99.99	99.99	19.80	99.99	?
PM I13265-1558	201.631165	-15.979954	0.505	-0.505	-0.011	34.9	0.011	18.4	17.9	17.9	99.99	99.99	99.99	18.17	99.99	?
PM I13306-2039	202.670593	-20.650953	0.591	0.316	-0.499	39.8	0.010	13.6	11.5	9.4	8.28	7.65	7.39	12.63	4.35	d
PM I13317-6305	202.947296	-63.085049	0.626	-0.609	0.147	6.3	0.063	99.8	16.1	13.6	13.71	13.17	12.92	17.20	3.49	sd
PM I13332-6751	203.310654	-67.854759	0.795	-0.743	-0.283	12.9	0.031	17.7	16.7	16.0	15.37	15.20	13.37	17.24	1.87	wd
PM I13334-1503	203.355637	-15.061091	0.548	-0.457	-0.302	28.8	0.014	19.4	16.8	14.8	13.27	12.84	12.45	18.20	4.93	d
PM I13341-7121	203.547928	-71.364250	0.502	-0.376	-0.333	12.9	0.031	15.9	13.4	11.5	10.10	9.51	9.20	14.75	4.65	d
PM I13351-1037	203.794006	-10.618372	0.464	-0.160	0.436	36.8	0.011	20.6	18.5	18.2	17.42	16.11	15.50	19.63	2.21	wd
PM I13506-6847	207.663071	-68.788033	0.746	-0.595	-0.450	12.9	0.031	14.6	13.1	12.0	11.29	10.69	10.40	13.91	2.62	sd
PM I14223-7023	215.581116	-70.393639	0.819	-0.726	-0.380	13.1	0.031	16.5	13.6	11.2	10.23	9.67	9.37	15.17	4.94	d
PM I14309-6728	217.735794	-67.478683	0.564	-0.436	-0.358	10.3	0.039	17.5	15.6	14.0	12.24	11.69	11.40	16.63	4.39	d

TABLE 2 — *Continued*

Star	α (ICRS)	δ (ICRS)	μ ($''$ yr $^{-1}$)	μ_α ($''$ yr $^{-1}$)	μ_δ ($''$ yr $^{-1}$)	Δr^a (yr)	μ_{err}^b ($''$ yr $^{-1}$)	B_J^c	R_F	I_N	J^d	K	H	V	$V-J$	class
PM I14460-1518	221.509415	-15.304267	0.465	-0.463	0.046	39.0	0.010	20.5	18.9	15.6	13.45	12.88	12.57	19.76	6.31	d
PM I14521-7157	223.025345	-71.962532	0.491	-0.465	-0.159	13.1	0.031	17.6	15.8	13.5	12.30	11.82	11.50	16.77	4.47	d
PM I14537-4820	223.430466	-48.345669	0.501	-0.487	-0.116	13.2	0.030	18.6	16.2	16.0	14.80	14.15	14.05	17.50	2.70	sd
PM I15066-4230	226.673096	-42.515308	0.547	-0.546	-0.036	16.8	0.024	17.8	17.5	17.5	11.67	11.19	10.85	17.66	5.99	d
PM I15144-5753	228.623672	-57.888840	0.479	-0.340	-0.337	18.7	0.021	12.0	10.7	11.5	9.47	8.57	8.27	11.34	1.87	sd
PM I15181-6058	229.531143	-60.968319	0.546	-0.293	-0.461	13.6	0.029	14.0	13.1	10.9	10.11	9.48	9.27	14.20	4.09	d
PM I15217-2713	230.442184	-27.217743	0.594	-0.323	-0.499	14.9	0.027	16.6	14.5	13.4	11.80	11.34	11.08	15.63	3.83	d
PM I15229-0244	230.747040	-2.748156	0.611	-0.524	-0.314	34.2	0.012	20.6	17.6	15.6	14.28	13.80	13.46	19.22	4.94	d
PM I15499-5524	237.478027	-55.416222	0.564	-0.500	-0.261	10.6	0.038	17.1	15.6	13.5	12.63	12.06	11.75	16.41	3.78	sd
PM I15562-2221	239.074875	-22.365160	0.488	-0.269	-0.407	37.3	0.011	15.9	14.5	13.4	12.10	11.60	11.37	15.26	3.16	sd
PM I16006-1654	240.171509	-16.908398	0.812	-0.786	0.205	41.9	0.010	19.1	17.5	17.3	16.56	16.27	16.57	18.36	1.80	wd
PM I16230-6905	245.761459	-69.093605	1.594	-1.005	-1.237	17.0	0.024	17.5	15.2	99.8	11.38	10.86	10.53	16.44	5.06	d
PM I16336-3713	248.404129	-37.220367	0.521	-0.517	-0.068	10.8	0.037	16.5	15.8	15.8	15.02	14.54	14.34	16.18	1.16	wd
PM I16389-5555	249.743118	-55.918385	0.642	-0.427	-0.480	12.0	0.033	16.9	14.8	14.1	13.74	13.23	13.00	15.93	2.19	sd
PM I16507-2813	252.689224	-28.231855	0.535	-0.361	-0.395	13.2	0.030	17.4	13.2	12.0	10.69	10.16	9.93	15.47	4.78	d
PM I16522-2237	253.058136	-22.624069	0.646	-0.262	-0.591	38.9	0.010	16.4	14.5	13.9	12.93	12.39	12.17	15.53	2.60	sd
PM I16527-2913	253.180145	-29.218122	0.484	-0.298	-0.382	13.2	0.030	17.2	15.8	14.0	13.28	12.70	12.53	16.56	3.28	sd
PM I16585-1016	254.635452	-10.281461	0.654	-0.298	-0.582	37.8	0.011	20.4	18.4	17.1	99.99	99.99	99.99	19.48	99.99	?
PM I17004-2207	255.116562	-22.129393	0.503	-0.086	-0.496	38.9	0.010	16.2	13.6	11.4	10.22	9.64	9.40	15.00	4.78	d
PM I17020-3835	255.506058	-38.598938	0.562	-0.204	-0.524	14.1	0.028	18.1	16.0	14.5	14.14	13.67	13.54	17.13	2.99	sd
PM I17032-3104	255.809204	-31.081165	0.561	-0.226	-0.513	13.2	0.030	16.3	15.1	13.2	12.52	12.00	11.75	15.75	3.23	sd
PM I17042-3639	256.069702	-36.664280	0.514	-0.037	-0.513	11.2	0.036	16.2	14.7	12.7	11.53	11.02	10.78	15.51	3.98	d
PM I17044-2154	256.123749	-21.902493	0.665	-0.501	-0.437	39.6	0.010	17.1	15.1	14.0	13.46	12.93	12.75	16.18	2.72	sd
PM I17046-1257	256.170166	-12.953110	0.674	-0.512	-0.439	36.9	0.011	17.5	15.3	14.9	13.62	13.09	12.90	16.49	2.87	sd
PM I17049-0257	256.238464	-2.951268	0.493	0.124	-0.477	38.1	0.010	16.0	15.9	15.9	15.87	15.75	15.73	15.95	0.08	wd
PM I17059-2030	256.479004	-20.514038	0.706	-0.539	-0.456	37.8	0.011	17.8	15.1	13.2	13.42	12.92	12.80	16.56	3.14	sd
PM I17076-2502	256.900452	-25.042465	0.639	-0.204	-0.606	39.9	0.010	16.0	13.5	12.0	11.49	10.97	10.77	14.85	3.36	d
PM I17082-3436	257.061646	-34.606270	0.861	-0.323	-0.798	11.2	0.036	99.8	13.1	10.8	10.87	10.36	10.01	14.20	3.33	sd
PM I17084-2209W	257.106445	-22.156849	0.513	-0.368	-0.358	39.6	0.010	17.7	15.5	13.0	12.92	12.45	12.21	16.80	3.88	d
PM I17084-2209E	257.107391	-22.157591	0.513	-0.368	-0.358	39.6	0.010	17.9	15.7	13.1	13.52	13.04	12.79	16.78	3.26	sd
PM I17088-2105	257.215820	-21.087744	0.890	-0.769	-0.448	39.6	0.010	18.2	15.2	13.6	12.23	11.77	11.49	16.82	4.59	d
PM I17105-3440	257.626434	-34.671501	0.521	0.101	-0.511	11.2	0.036	19.2	17.0	15.6	13.55	13.06	12.77	18.19	4.64	d
PM I17118-1335	257.969330	-13.593397	0.886	-0.488	-0.740	32.9	0.012	15.6	13.5	12.5	10.95	10.46	10.18	14.63	3.68	d
PM I17137-4535	258.431580	-45.599136	0.466	-0.143	-0.444	11.9	0.034	17.5	16.1	15.4	14.42	13.92	13.74	16.86	2.44	sd
PM I17140-2728	258.518677	-27.477440	0.471	-0.373	-0.287	13.0	0.031	18.5	17.0	16.7	14.93	13.93	13.35	17.81	2.88	sd
PM I17182-1019	259.552765	-10.324768	0.489	-0.269	-0.408	35.0	0.011	18.0	16.5	14.3	12.25	11.66	11.33	17.31	5.06	d
PM I17189-4131	259.727539	-41.527756	1.160	0.964	-0.645	11.8	0.034	16.4	15.4	12.9	10.61	10.00	9.62	15.94	5.33	d
PM I17195-1230	259.886536	-12.501122	0.493	0.050	-0.490	35.0	0.011	16.2	14.8	12.7	11.27	10.76	10.45	15.56	4.29	d
PM I17224-1938	260.611664	-19.639271	0.633	-0.322	-0.545	37.9	0.011	17.6	13.6	12.1	11.06	10.57	10.23	15.76	4.70	d
PM I17238-3541	260.962982	-35.686134	0.569	-0.136	-0.552	11.2	0.036	15.6	13.5	11.4	10.07	9.49	9.22	14.63	4.56	d
PM I17265-2342	261.632538	-23.714851	0.640	-0.341	-0.542	42.0	0.010	18.4	16.0	14.2	14.34	13.84	13.64	17.30	2.96	sd
PM I17265-5102	261.641815	-51.046822	0.511	-0.245	-0.449	13.2	0.030	15.3	13.8	12.2	11.32	10.77	10.55	14.61	3.29	d
PM I17273-4851	261.833893	-48.866642	0.610	-0.211	-0.572	13.2	0.030	99.8	14.1	12.9	12.72	12.25	12.06	14.83	2.11	sd
PM I17324-4239	263.121307	-42.657875	0.559	-0.534	-0.165	11.8	0.034	15.8	14.1	13.0	12.23	11.69	11.51	15.02	2.79	sd
PM I17364-3605	264.113586	-36.096539	0.932	-0.390	-0.846	9.7	0.041	14.2	12.9	11.4	10.27	9.76	9.52	13.60	3.33	d
PM I17386-3427	264.654999	-34.458603	0.491	-0.301	-0.388	9.7	0.041	99.8	14.1	13.3	10.82	10.24	9.98	15.20	4.38	d
PM I17394-2327	264.851440	-23.452009	0.491	-0.485	-0.074	11.0	0.036	17.7	13.5	11.7	10.62	10.03	9.78	15.77	5.15	d
PM I17436-2303	265.905365	-23.066505	0.487	-0.080	-0.480	11.0	0.036	17.1	14.1	12.4	11.93	11.25	11.03	15.72	3.79	d
PM I17444-2044	266.121948	-20.747021	0.736	-0.240	-0.696	41.1	0.010	16.8	13.9	12.3	11.31	10.77	10.60	15.47	4.16	d
PM I17468-0346	266.711670	-3.769525	0.535	-0.425	-0.325	35.0	0.011	18.3	16.8	15.5	14.49	13.99	13.89	17.61	3.12	sd
PM I17476-5436	266.903381	-54.608665	0.462	-0.392	-0.244	3.0	0.133	15.7	15.3	14.4	14.46	14.22	14.29	15.52	1.06	wd
PM I17480-5043	267.012421	-50.728275	0.577	-0.200	-0.541	13.2	0.030	17.3	15.3	13.5	12.55	12.02	11.81	16.38	3.83	d
PM I17489-4002	267.232697	-40.039345	0.523	-0.289	-0.436	12.3	0.033	15.1	13.8	12.5	12.35	11.83	11.64	14.50	2.15	sd
PM I17509-2734	267.727722	-27.576120	0.533	-0.403	-0.349	11.0	0.036	15.5	13.3	13.4	11.73	11.21	10.95	14.49	2.76	sd
PM I17521-3916	268.046082	-39.281761	0.491	-0.130	-0.473	12.3	0.033	15.8	14.8	13.1	11.83	11.24	10.99	15.34	3.51	d
PM I17525-0248	268.140717	-2.811024	0.530	-0.063	-0.526	30.0	0.013	16.6	14.8	13.2	12.10	11.58	11.37	15.77	3.67	d

170 New Southern Stars with $\mu > 0.45''\text{yr}^{-1}$

TABLE 2 — *Continued*

Star	α (ICRS)	δ (ICRS)	μ (" yr ⁻¹)	μ_α (" yr ⁻¹)	μ_δ (" yr ⁻¹)	Δr^a (yr)	μ_{err}^b (" yr ⁻¹)	B_J^c	R_F	I_N	J^d	K	H	V	$V-J$	class
PM I17540-3440	268.512390	-34.671764	0.639	-0.465	-0.438	10.0	0.040	15.2	12.9	11.6	9.43	8.88	8.55	14.14	4.71	d
PM I17595-1755	269.885742	-17.926767	1.143	-0.410	-1.067	37.0	0.011	15.5	13.9	13.0	11.44	10.94	10.69	14.76	3.32	sd
PM I18018-2706	270.469421	-27.115088	0.557	-0.243	-0.501	41.1	0.010	16.2	13.2	12.8	10.51	9.90	9.60	14.82	4.31	d
PM I18044-1005	271.117157	-10.091301	0.483	-0.283	-0.392	34.2	0.012	17.0	14.7	99.8	11.41	10.84	10.53	15.94	4.53	d
PM I18063-1913	271.575317	-19.224737	0.851	-0.557	-0.643	37.1	0.011	17.2	14.4	14.4	12.95	12.38	12.15	15.91	2.96	sd
PM I18087-2632	272.198090	-26.544395	0.559	-0.322	-0.457	12.2	0.033	14.7	12.9	99.8	10.30	9.73	9.49	13.87	3.57	d
PM I18088-7042	272.223938	-70.707069	0.523	0.213	-0.478	14.9	0.027	18.4	16.3	15.8	15.74	15.37	15.41	17.43	1.69	wd
PM I18094-4104	272.352509	-41.076588	0.481	0.237	-0.419	12.0	0.033	16.0	14.6	12.9	11.43	10.90	10.61	15.36	3.93	d
PM I18095-3012	272.376709	-30.205776	0.486	-0.374	-0.310	11.8	0.034	13.7	12.6	11.0	10.46	9.91	9.69	13.19	2.73	d
PM I18106-0650	272.667755	-6.848365	0.484	-0.136	-0.464	34.1	0.012	16.0	14.0	12.9	12.07	11.51	11.39	15.08	3.01	sd
PM I18118-1419	272.950073	-14.325014	0.455	-0.445	-0.095	34.1	0.012	19.6	17.3	17.0	15.21	13.87	13.38	18.54	3.33	sd
PM I18177-1302	274.440796	-13.045858	0.483	-0.301	-0.378	32.2	0.012	18.6	16.0	14.8	13.35	12.67	11.83	17.40	4.05	d
PM I18200-3828	275.012390	-38.472858	0.747	-0.335	-0.668	12.0	0.033	15.5	13.9	12.3	10.92	10.39	10.13	14.76	3.84	d
PM I18244-2521	276.123779	-25.352663	0.642	-0.318	-0.558	12.2	0.033	14.9	14.7	11.4	10.66	10.01	9.74	14.81	4.15	d
PM I18265-1923	276.631653	-19.391891	0.552	-0.282	-0.474	39.9	0.010	14.4	12.9	11.0	9.77	9.17	8.92	13.71	3.94	d
PM I18292-3059S	277.319672	-30.998821	0.484	0.457	-0.158	11.8	0.034	99.8	12.5	99.8	10.67	10.16	9.94	13.50	2.83	d
PM I18292-3059N	277.320496	-30.996946	0.484	0.457	-0.158	11.8	0.034	99.8	12.4	99.8	10.25	9.77	9.49	13.50	3.25	d
PM I18310-2939	277.770935	-29.661570	0.750	-0.051	-0.748	11.8	0.034	14.6	13.3	11.3	10.34	9.86	9.59	14.00	3.66	d
PM I18429-1639	280.734833	-16.656038	0.473	-0.369	-0.296	35.6	0.011	16.4	16.1	12.7	12.34	11.87	11.57	16.26	3.92	d
PM I18456-2337	281.405945	-23.630495	0.646	0.214	-0.609	11.9	0.034	17.1	14.5	13.5	11.51	10.97	10.73	15.90	4.39	d
PM I18530-1533	283.269012	-15.551133	0.506	-0.091	-0.498	33.0	0.012	15.8	14.2	13.2	11.19	10.70	10.48	15.06	3.87	d
PM I18533-2556	283.332947	-25.945759	0.493	-0.302	-0.390	41.8	0.010	20.3	18.0	16.6	15.29	14.73	14.53	19.24	3.95	sd
PM I18536-2305	283.417114	-23.090977	0.455	0.361	-0.277	11.9	0.034	18.5	15.9	16.6	14.87	14.42	14.07	17.30	2.43	sd
PM I19068-2414	286.706268	-24.245245	0.655	0.097	-0.648	3.8	0.105	17.4	15.7	14.2	12.64	12.13	11.91	16.62	3.98	sd
PM I19072-1931	286.819061	-19.531000	0.562	-0.277	-0.489	37.0	0.011	18.0	16.4	15.1	14.73	14.24	14.10	17.26	2.53	sd
PM I19131-1151	288.280762	-11.862134	0.598	-0.121	-0.586	36.7	0.011	16.0	13.8	12.4	11.08	10.49	10.33	14.99	3.91	d
PM I19163-2322	289.096924	-23.375906	0.572	0.251	-0.514	37.0	0.011	16.8	13.9	11.2	10.20	9.63	9.33	15.47	5.27	d
PM I19316-0658	292.911163	-6.973796	0.544	-0.143	-0.525	34.7	0.012	15.2	12.8	10.6	9.48	8.77	8.58	14.10	4.62	d
PM I19334-1434	293.372406	-14.580217	0.886	-0.571	-0.677	34.0	0.012	14.0	12.3	11.4	10.63	10.07	9.85	13.22	2.59	sd
PM I19350-0725	293.756409	-7.424497	0.718	0.536	-0.477	33.7	0.012	17.1	14.9	13.6	12.03	11.53	11.25	16.09	4.06	d
PM I19394-1016	294.851349	-10.280749	0.466	-0.252	-0.392	35.9	0.011	18.5	16.5	15.1	13.88	13.38	13.17	17.58	3.70	sd
PM I19418-0208	295.470551	-2.146091	1.093	-0.282	-1.056	35.1	0.011	18.0	16.9	16.6	14.62	14.14	13.99	17.49	2.87	sd
PM I19427-1723	295.680054	-17.390104	0.904	0.028	-0.904	35.1	0.011	14.1	13.0	10.6	9.83	9.26	8.98	13.59	3.76	d
PM I19428-0304	295.700165	-3.075746	0.868	-0.549	-0.672	31.9	0.013	18.6	16.4	14.7	13.98	13.45	13.25	17.59	3.61	sd
PM I19484-5101	297.117523	-51.025124	0.690	0.190	-0.663	15.2	0.026	99.8	16.1	13.9	12.46	11.98	11.68	17.20	4.74	d
PM I19578-2513	299.468140	-25.225792	0.599	-0.092	-0.591	15.1	0.026	18.8	17.9	16.9	15.24	14.99	14.78	18.39	3.15	sd
PM I20079-4205	301.980164	-42.087429	0.771	0.044	-0.770	17.1	0.023	15.5	13.6	10.9	9.52	8.96	8.61	14.63	5.11	d
PM I20138-0216	303.468933	-2.272357	0.498	-0.133	-0.480	37.0	0.011	19.3	16.3	14.6	13.00	12.52	12.23	17.92	4.92	d
PM I20205-4202	305.128723	-42.048962	0.473	0.135	-0.453	14.6	0.027	16.7	16.3	16.5	16.34	15.98	15.86	16.52	0.18	wd
PM I20271-4421	306.779480	-44.358181	0.550	0.178	-0.520	13.9	0.029	15.0	13.3	11.5	10.08	9.48	9.16	14.40	4.32	d
PM I20278-4301	306.956390	-43.020847	0.823	0.199	-0.799	13.9	0.029	17.9	16.7	16.5	15.85	15.61	15.61	17.35	1.50	wd
PM I20289-5004	307.243835	-50.071632	0.484	0.279	-0.396	14.9	0.027	14.0	12.9	11.8	11.04	10.46	10.26	13.92	2.88	d
PM I20335-3735	308.389313	-37.595295	0.528	0.513	-0.125	14.6	0.027	19.3	17.1	14.6	12.74	12.21	11.86	18.29	5.55	d
PM I20347-3630	308.678497	-36.515709	0.693	0.189	-0.667	15.2	0.026	99.8	15.3	99.8	12.27	11.82	11.54	16.40	4.13	d
PM I20348-6347	308.720459	-63.795998	0.452	0.238	-0.384	15.0	0.027	14.5	12.1	10.6	9.37	8.76	8.51	13.40	4.03	d
PM I20457-1411	311.429321	-14.192146	0.814	0.157	-0.799	31.8	0.013	20.5	17.5	99.8	15.10	14.57	14.57	19.12	4.02	sd
PM I20457-3013	311.448883	-30.223770	0.512	0.512	-0.009	16.2	0.025	17.8	15.9	13.5	11.77	11.22	10.91	16.93	5.16	d
PM I20502-3424	312.567383	-34.411858	0.533	0.360	-0.393	14.9	0.027	14.8	12.8	10.4	8.82	8.27	8.00	13.88	5.06	d
PM I20589-3457	314.743744	-34.952717	0.687	0.339	-0.597	14.9	0.027	15.1	13.8	13.2	11.96	11.52	11.38	14.50	2.54	sd
PM I21023-6046	315.592163	-60.771648	0.560	0.168	-0.534	15.1	0.026	19.6	17.6	17.0	15.63	15.20	14.83	18.68	3.05	sd
PM I21163-3303	319.076721	-33.063358	0.768	0.712	-0.289	14.9	0.027	99.8	15.9	13.9	12.39	11.86	11.58	17.00	4.61	d
PM I21340-1413	323.510071	-14.228679	0.648	-0.314	-0.567	33.2	0.012	20.6	18.3	15.6	13.99	13.43	13.11	19.54	5.55	d
PM I21349-0500	323.736084	-5.015940	0.466	-0.306	-0.351	31.1	0.013	18.0	17.5	16.8	16.70	16.03	16.28	17.77	1.07	wd
PM I21356-3448	323.910217	-34.812588	0.639	0.626	-0.127	15.1	0.026	15.8	13.9	12.2	11.20	10.67	10.44	14.93	3.73	d
PM I21375-1014	324.379944	-10.240491	0.625	0.181	-0.598	34.2	0.012	16.1	14.1	99.8	10.26	9.73	9.43	15.18	4.92	d
PM I22033-2359	330.843201	-23.995905	0.513	0.503	-0.102	14.1	0.028	18.5	16.9	14.4	12.53	12.00	11.66	17.76	5.23	d

TABLE 2 — *Continued*

Star	$\alpha(\text{ICRS})$	$\delta(\text{ICRS})$	μ ($'' \text{yr}^{-1}$)	μ_α ($'' \text{yr}^{-1}$)	μ_δ ($'' \text{yr}^{-1}$)	Δt^a (yr)	μ_{err}^b ($'' \text{yr}^{-1}$)	B_J^c	R_F	I_N	J^d	K	H	V	$V-J$	class
PM I23035-2809	345.884521	-28.157280	0.464	0.463	0.016	14.1	0.028	20.3	17.0	15.6	13.61	13.06	12.80	18.78	5.17	d
PM I23187-3135	349.684784	-31.583717	0.511	0.456	-0.229	19.0	0.021	19.8	16.7	99.8	99.99	99.99	99.99	18.37	99.99	?
PM I23440-8246	356.014435	-82.782303	0.694	0.694	-0.022	18.8	0.021	17.2	16.6	16.6	15.97	15.73	15.53	16.92	0.95	wd

^a Temporal baseline between the first and second DSS epoch.

^b Estimated proper motion error.

^c Photographic B_J (IIIaJ), R_F (IIIaF) and I_N (IVN) magnitudes from the USNO-B1.0 catalog.

^d Infrared JHK_s magnitudes from the 2MASS All-Sky Point Source Catalog.